NASA Contractor Report CR-2002-211181

Final Report on Land-Breeze Forecasting

Prepared By:
Jonathan L. Case
Applied Meteorology Unit

Prepared for:
Kennedy Space Center
Under Contract NAS10-01052

NASA
National Aeronautics and
Space Administration

Office of Management

Scientific and Technical
Information Program

2002

Attributes and Acknowledgments

NASA/KSC POC:
Dr. Francis J. Merceret
YA-D

Applied Meteorology Unit (AMU)
Jonathan L. Case
Mark M. Wheeler

Executive Summary

The nocturnal land breeze at the Kennedy Space Center (KSC) and Cape Canaveral Air Force Station (CCAFS) is both operationally significant and challenging to forecast. The occurrence and timing of land breezes impact low-level winds, atmospheric stability, low temperatures, and fog development. Accurate predictions of the land breeze are critical for toxic material dispersion forecasts associated with space launch missions, since wind direction and low-level stability can change noticeably with the onset of a land breeze.

This report presents a seven-year observational study of land breezes over east-central Florida from 1995 to 2001. This comprehensive analysis was enabled by the high-resolution tower observations over KSC/CCAFS. Five-minute observations of winds, temperature, and moisture along with 915-MHz Doppler Radar Wind Profiler data were used to analyze specific land-breeze cases, while the tower data were used to construct a composite climatology. Utilities derived from this climatology were developed to assist forecasters in determining the land-breeze occurrence, timing, and movement based on predicted meteorological conditions.

An objective algorithm was designed to identify onshore to offshore wind-shift lines across KSC/CCAFS in order to develop a seven-year climatology of land breezes. To be defined as a land breeze, the algorithm ensured that offshore winds prevailed behind the boundary and that the wind shift tracked eastward towards the coast. To enable this objective land-breeze identification, the 54-ft winds at all KSC/CCAFS towers were interpolated to a high-resolution analysis grid every five minutes using an objective analysis technique. The algorithm incorporated a number of preliminary meteorological checks to prevent false identifications of frontal passages or outflow boundaries as land breezes. All events identified by the algorithm were validated manually, and the vertical structure of each event that impacted the tallest tower in the network was analyzed. In addition, the occurrence or absence of a sea breeze was noted for each afternoon before a land breeze.

Some key results found during the seven years of study include the following:

- Land breezes were found to occur in any month of the year under certain meteorological conditions, and had widely varying depths and onset times.
- There were 393 land-breeze events identified and validated, 248 during the minimal convective months of October to May, and 145 during the peak convective months of June to September.
- Land breezes were most common during the months of April, May, July, and August, and were least common during December and January.
- The onset times had a large amount of variability, but were typically earliest from May to July (~ 4 to 5 hours after sunset) and latest from October to January (~ 6.5 to 8 hours after sunset).
- Land breezes typically moved from the west or southwest during April to August, and predominantly from the northwest in October and November. Land breezes were equally common from all directions in the winter months.
- Fog was much more common during nights with land breezes throughout the year.
- From October to May, the passage of a land-breeze front led to a decrease in 54-ft temperatures, and often an increase in 6-ft temperatures, resulting in a decrease of the near-surface stability. The land breeze had a negligible impact on low-level temperatures and stability in the summer.

For land breezes that affected Tower 313, the circulation depth was classified as either deep (> 492 ft) or shallow (< 492 ft). Land breezes with deep circulations had an average onset time about four hours earlier than shallow circulations during all parts of the year (~ 4.5 versus 8.5 hours after sunset). Over 80% of the deep events were associated with a sea breeze during the preceding afternoon, whereas less than 40% of shallow events had a preceding sea breeze. The earlier onset time combined with the large number of preceding sea breezes suggest that the deep land breezes were largely composed of coastward retreating sea breezes whereas the shallow land breezes were probably separate features not connected with the sea-breeze circulation.

Forecasters are provided with several utilities to assist in predicting the occurrence, onset time, and direction of movement of a land breeze on a given night. Flowcharts were developed to help forecasters determine the qualitative and quantitative probabilities of a land-breeze occurrence on a particular night based on meteorological criteria. In addition, if a land breeze is possible, forecasters will also have tables providing them with the most likely ranges of onset times based on the prevailing synoptic flow, month of the year, and occurrence or absence of a sea breeze during the day. Finally, forecasters are provided with diagrams that relate the synoptic flow direction to the land-breeze direction based on the results from the seven-year

composite data. These tools will help forecasters to determine land-breeze occurrence more consistently and predict the timing and movement of land breezes with increased confidence and accuracy.

Table of Contents

List of Figures

List of Tables

1. Introduction

1.1 Motivation

The onset of a land breeze at the Kennedy Space Center (KSC) and Cape Canaveral Air Force Station (CCAFS) is both operationally significant and challenging to forecast. The occurrence and timing of the nocturnal land breeze impact low-level winds, atmospheric stability, low temperatures, and fog development. Accurate predictions of the land breeze are especially critical for toxic material dispersion forecasts associated with space launch missions, since wind direction and low-level stability can change noticeably with the passage of a land-breeze front.

The U.S. Air Force 45th Weather Squadron (45 WS) forecasters find it challenging to determine the onset time and strength of the land breeze when it occurs. Several studies have analyzed the sea-breeze phenomena in great detail; however, limited work has been done to examine the characteristics, structure, and evolution of land breezes, while virtually no work exists on forecasting land breezes. As a result, the Applied Meteorology Unit (AMU) was tasked to analyze the characteristics of the land breeze at KSC/CCAFS and develop forecast tools. The AMU was also tasked to develop an automated tool that could consist of a decision tree, multiple discriminate analysis, regression equations, or other statistical tool, if possible. The ultimate goal is to improve the reliability of the occurrence forecasts and help determine the timing, duration, speed, and direction of the land breeze.

1.2 Background Information and Previous Studies

The theory behind land breezes is that they are driven by nocturnal thermal contrasts between the land and water, similar to the sea breeze. Since the land cools faster than the nearby ocean, a shallow mesoscale pressure gradient develops, with higher surface pressure over the land compared to the water. The resulting circulation is directed from the land to the sea near the surface (e.g. the land breeze) along with a corresponding return flow from sea to land above the land breeze. The land-breeze circulation is generally weaker than the sea breeze in both velocity and height of development since the surface-based heat source for the land breeze (e.g. ocean) is much weaker than the heat source for the sea-breeze circulation (e.g. land, Atkinson 1981).

Many recent studies have focused on the observational aspects of the sea-breeze phenomena over the Florida peninsula from the Convection and Precipitation/Electrification experiment (Wakimoto and Atkins 1994; Atkins et al. 1995; Kingsmill 1995; Laird et al. 1995; Atkins and Wakimoto 1997; Wilson and Megenhardt 1997). Several studies have also addressed other aspects of sea breezes such as the influence of the prevailing large-scale flow (Arritt 1993), the diurnal evolution of the sea breeze (Simpson 1996), and the spatial and temporal variations of the leading front as observed by an aircraft (Stephan et al. 1999). Very few projects have examined the land-breeze phenomena in detail, particularly over flat terrain such as the Florida peninsula.

The only studies found that compiled a land-breeze climatology are Sen Gupta and Chakravortty (1947, hereafter SC47) and Dekate (1968), both conducted in India and rather dated. In SC47, the authors compiled a five-year climatology of land breezes at Calcutta, which consisted of monthly onset time frequencies, duration, wind direction, and temperature and humidity changes associated with the land breeze. Meanwhile, Dekate (1968) compiled the monthly average frequency and onset times of both land and sea breezes in Bombay, with a primary emphasis on the sea breeze. The SC47 study has the greatest relevance to the current AMU task, since Calcutta is much closer to the latitude of Cape Canaveral, FL and the terrain of Calcutta more closely resembles the terrain of east-central Florida. The dearth in land-breeze studies is not surprising since the phenomenon does not often lead to convective initiation as with the sea breeze.

The studies most applicable to this task are Zhong and Takle (1992, hereafter ZT92) and Zhong and Takle (1993, hereafter ZT93). Using observational data from the KSC Atmospheric Boundary Layer Experiment (Taylor et al. 1990), ZT92 examined the evolution of a sea and land breeze in late May 1989. Based their findings, the authors suggested that the mesoscale pressure gradient was much less important in forcing the land breeze compared to the sea breeze. In their companion paper, ZT93 conducted experiments using a boundary-layer model to determine the sea and land-breeze evolution and balance of forces under various large-scale wind regimes. From these experiments, the authors found that an onshore wind greater than 10 kt prevented the development of a land breeze. Furthermore, ZT93 concluded that the strength of the land breeze was more

sensitive to the prevailing large-scale flow and daytime surface heating compared to the magnitude of the nocturnal surface cooling over land. Their findings, along with the results in this report, serve to refute the traditional notion that the land breeze is solely driven by thermal contrasts between the land and the sea.

1.3 Report Format and Outline

This report presents the first multi-year observational study of land breezes over east-central Florida. This comprehensive analysis was enabled by the high-resolution tower network over KSC/CCAFS. Five-minute observations of winds, temperature, and moisture along with 915-MHz Doppler Radar Wind Profiler (DRWP) data were used to analyze specific land-breeze cases, while the tower data were used to construct a composite climatology.

The report is organized as follows. Section 2 describes the data and methodology used to develop a seven-year land-breeze climatology over KSC/CCAFS, and the data used to examine relationships for possible forecast tools. Section 3 presents an analysis of sample land-breeze events from March and April 2000 using KSC/CCAFS tower and 915-MHz DRWP data. The results of the land-breeze climatology are presented in Section 4. A summary of the conditions favorable for land-breeze development, along with forecast tools for determining the land-breeze onset time and movement is given in Section 5. Finally, Section 6 summarizes the report and provides direction for future analysis to improve the predictability of the land breeze.

2. Data and Methodology

The ultimate goal of this task was to develop forecast guidance and/or an automated tool to improve 45 WS land-breeze predictions for a given night. The first step towards realizing such a tool was to obtain a good understanding of the land breeze and its behavior at KSC/CCAFS. As a result, several individual land-breeze events for an entire cool season were subjectively examined to understand the meteorological conditions associated with the land-breeze passages. A seven-year climatology of land breezes across east-central Florida was then constructed, focusing on events with sharp wind shifts (e.g. at least 20° direction change over a 1.4-nm distance) using an objective technique to identify onshore to offshore wind shifts propagating east towards the coast. Based on the results of the climatology and the ZT92 and ZT93 findings, several parameters that have potential to provide forecast guidance in predicting land breezes were then examined. The observational data sets and details of the methodology used to develop the climatology and forecast tools are provided in the following sub-sections.

2.1 Data Sets

Four observational data sets were used to analyze land breezes and develop a multi-year climatology:

- KSC/CCAFS towers,
- KSC/CCAFS 915-MHz DRWPs,
- Mean sea level pressure (MSLP) analyses, and
- Archived surface observations from the Shuttle Landing Facility (TTS).

These data sets are described in detail in the following sub-sections, along with the quality control method used.

2.1.1 KSC/CCAFS towers and quality control method

The data set used to study land breezes and develop the climatology is the KSC/CCAFS mesonet of 44 observational towers (Fig. 2.1). The KSC/CCAFS mesonet has an average station spacing of 2.7 nm (5 km) and measures temperature, dew point, and winds at various levels ranging from 6 ft to 492 ft. The primary measurement levels for most towers are 6 ft (temperature and dew point), 12 ft (winds), and 54 ft (winds and temperature). This study uses the 6-ft temperature and humidity, 54-ft wind and temperature, and the difference between the 6-ft and 54-ft temperatures for near-surface stability. The archived 5-minute tower data were used for this study and provided by Computer Science Raytheon.

All KSC/CCAFS tower data were subject to quality control (QC) prior to analysis and processing for the land-breeze climatology. The QC method included five routines consisting of an unrealistic value check, a standard deviation check, a peak-to-average wind speed ratio check, a vertical consistency check, and a temporal consistency check. More details on the QC algorithm can be found in Lambert (2002).

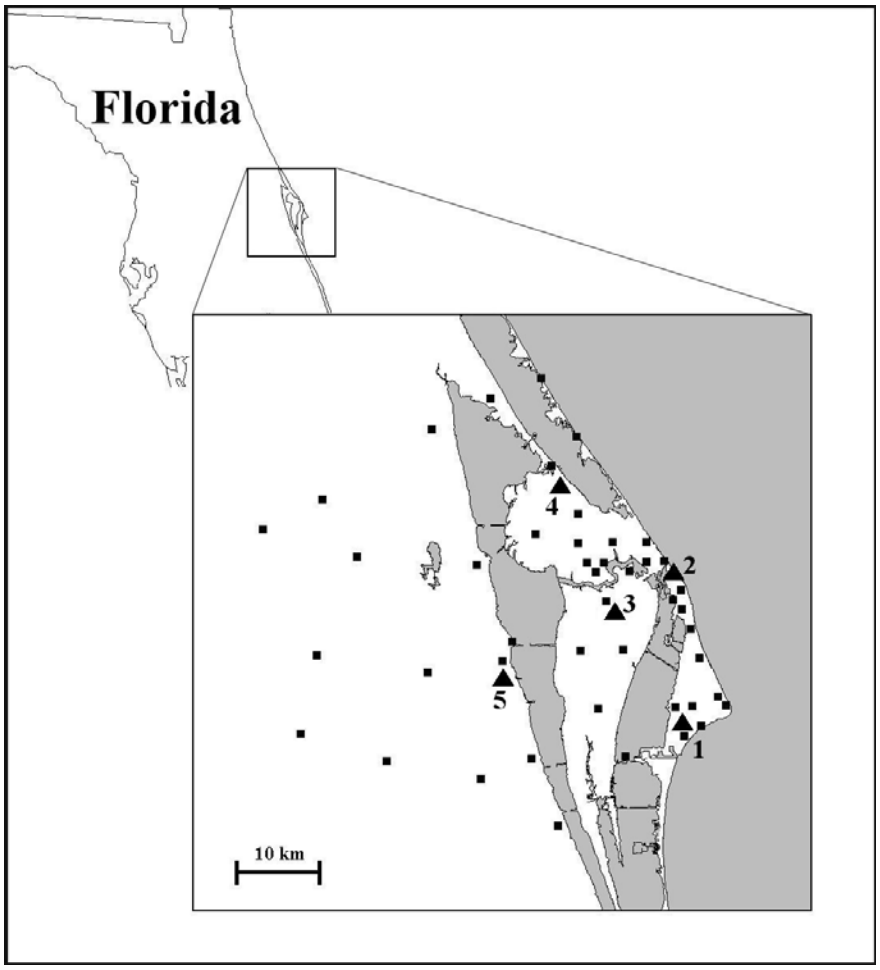

Figure 2.1. The locations of the 44 KSC/CCAFS observational towers (squares) used to study land breezes and develop the seven-year land-breeze climatology over east-central Florida. The locations of the five 915-MHz DRWP sensors are given by triangles and labeled with numbers 1–5.

2.1.2 915-MHz DRWP and quality control method

Archived 915-MHz DRWP data were used to supplement the subjective analysis of several individual land-breeze events. These data provide valuable boundary-layer wind information from 426 ft (130 m) to as high as 19685 ft (6000 m), depending on the meteorological conditions that affect the signal-to-noise ratio of the instrument. Under typical conditions, the 915-MHz profilers can measure wind data from 426 ft to approximately 10000 ft. The gate-to-gate resolution of the instrument is about 328 ft (100 m) and measurements are available every 15 minutes.

The 915-MHz DRWP data were subjected to a rigorous QC algorithm that includes several checks. A modified QC algorithm, developed by a colleague (Merceret 2002, personal communication) and based on the quality assessment routines described in Lambert and Taylor (1998), was applied to the 915-MHz DRWP data during the period from November 1999 to August 2001. The QC'd data were then used to examine the vertical structure of several land-breeze events that were at least 500 ft deep, above the top of the tallest tower.

2.1.3 Mean sea-level pressure reanalysis data

The National Centers for Environmental Prediction (NCEP) and National Center for Atmospheric Research (NCAR) have extensive reanalysis data dating back several decades (Kalnay et al. 1996). These data are available on a 2.5° latitude by 2.5° longitude grid and include many surface and upper-level meteorological

variables (refer to http://www.cdc.noaa.gov/cdc/data.nmc.reanalysis.html). For this project, the NCEP/NCAR reanalysis MSLP grids were utilized in two ways. First, contoured images of MSLP fields were obtained over a subset region that covers the southeastern United States and surrounding waters of the Gulf of Mexico and Atlantic Ocean. These contoured images were subjectively examined to classify the large-scale, synoptic flow associated with land-breeze days for developing the forecast tools described in Section 5. Second, the digital MSLP reanalysis data over this subset were downloaded and used by the objective technique to distinguish between land breezes and wind shifts associated with pressure troughs or fronts (see Section 2.3).

2.1.4 Shuttle Landing Facility hourly observations and quality control method

Hourly observations from TTS include standard atmospheric variables such as temperature, dew point, winds, MSLP, etc. As with the KSC/CCAFS towers and 915-MHz profilers, these data were subject to QC, according to the methods described by Lambert (2001). The QC routine consists of an unrealistic value check, a standard deviation check, and a temporal consistency check. These observations were used within the objective land-breeze identification technique as described in Section 2.3.

2.2 Subjective Analysis of Land-Breeze Events

The initial effort towards building the climatology was a subjective classification of events from the 1999–2000 cool season. The 1999–2000 cool season was chosen because the AMU had already documented all frontal/trough passages during these months as part of a previous model verification task (Case 2001).

To understand the characteristics of land breezes for constructing this climatology, all land breeze events were identified during the 1999–2000 cool season (October to April). Nights that experienced mean wind speeds less than ~10 kt (ZT93), mostly clear skies, and no frontal passages were prime candidates for identifying land breezes. Various characteristics of each land-breeze event were recorded such as the prevailing synoptic flow, the direction from which the land breeze originated, the onset time, and the length of time the land-breeze front was within the KSC/CCAFS tower network. In addition, several events were analyzed in detail, the results of which are presented in Section 3.

2.3 Objective Land-Breeze Identification Technique and Seven-Year Climatology

The subjective classification of all land-breeze events over several years would have been a labor-intensive task. Therefore, an objective, computer-based method was developed to identify land-breeze events without including other wind-shift lines such as fronts or precipitation outflows. The period of record used to develop the climatology spanned from February 1995 to January 2002. The starting month of February 1995 was chosen based on a format change in the archived tower data at that time.

The algorithm was designed to identify most land-breeze events while having a near zero false alarm rate (FAR). The algorithm was developed using the 1999–2000 cool-season data and attempted to match the results of the subjective land-breeze method as closely as possible. The program was then tested on the 1995–1996 cool-season data and results were validated by a manual examination of each day that the program classified a land breeze. Additional adjustments to the algorithm were made to remove false alarms.

In preparation for the objective algorithm, the KSC/CCAFS tower data were analyzed to a grid with 0.7-nm (1.25-km) horizontal grid spacing using the Barnes (1964) objective analysis technique. The temperature and dew point temperature at 6 ft, and temperature and u-/v-wind components at 54 ft were analyzed to the grid every 5 minutes.

The algorithm identified land-breeze boundaries from the analysis grids based on a distinct shift between onshore and offshore wind directions (defined in next paragraph), and tracked the boundary features across the grid. The program read in the gridded analysis data and computed the wind direction from the u-/v-wind components at each grid point in order to define a boundary separating onshore versus offshore winds. Prior to identifying and analyzing the movement of boundaries, several rules were applied to remove from consideration any nights that experienced meteorological conditions unfavorable for land-breeze development, or had too much missing data. The computer program eliminated nights in which any of the conditions listed in Table 2.1 occurred.

Table 2.1. A list of the meteorological and data conditions that warrant a night to be removed from consideration for a land breeze in the objective land-breeze identification program.

Condition	*Reason(s) for Rejection*
Presence of a trough in archived mean sea-level pressure (MSLP) data.	Prevent the identification of a wind shift associated with a frontal or trough passage.
Large MSLP changes (> 5.0 mb in 13 hours) at the Shuttle Landing Facility (TTS).	Prevent the identification of a wind shift associated with a frontal or trough passage.
Any report of precipitation at TTS between 0000 and 1300 UTC.	a) Avoid the identification of outflow boundaries. b) Occurrence of precipitation is highly unfavorable for land-breeze development.
More than 7 out of 14 hourly reports of cloud ceilings at TTS.	Insufficient radiational cooling for land-breeze development.
More than 5 out of a possible 14 TTS cloud reports missing.	Prevents the adequate determination of sufficiently clear skies (see condition above).
Mean nighttime, domain-wide 54-ft wind greater than 7 kt.	Wind speeds too strong for development of land breeze. This criterion was established based on the daily subjective analysis from October 1999 to April 2000.
More than 4% of 5-minute tower data missing between 0000 and 1300 UTC.	Too much missing data, preventing adequate temporal continuity for tracking boundaries in the program.

Boundary zones were identified according to wind-direction changes of at least 20° across a 1.4-nm distance (2.5 km, or two analysis grid zones). The wind direction was required to be onshore on the seaward side of the boundary and offshore on the landward side of the boundary. Offshore winds were given by wind directions between 180° and 335° and all other wind directions considered as onshore. These wind direction thresholds were chosen for two reasons. First, the coastline of east-central Florida is oriented approximately NNW to SSE (335°–155°) north of the tip of Cape Canaveral (refer to Fig. 2.1). Second, 180° rather than 155° was used to accommodate for the change in the coastline orientation to the south of Cape Canaveral and for the common inertial oscillation of winds (influence of the Coriolis force) over central Florida. During the subjective analysis of land breezes during the 1999–2000 developmental season, many land-breeze nights were found to have a gradual veering of the wind direction to southerly prior to the passage of the land-breeze front. This behavior was caused by the inertial oscillation, resulting in a nearly 360° clockwise turning of the wind direction at the latitude of KSC/CCAFS in about 50 hours (~ 7° h^{-1}) under benign weather conditions (ZT92).

Once the boundary points were flagged in the analysis grid, the land-breeze boundary start and stop times were identified based on time and space continuity and an empirically-determined minimum mean eastward movement of at least 4 nm (7.5 km, or six analysis grid zones). The start time is considered the onset time of the land breeze, or the time at which the program first identifies the boundary in the grid analysis domain. The stop time is the last time when the boundary is identified within the analysis domain, thus representing the time of the complete passage of the land-breeze front. To ensure temporal continuity, the boundary must be present at every 5-minute analysis time between the start and stop times. It is important to note that the offshore winds often prevailed for a few to several hours after the designated stop time of the land-breeze frontal passage.

Finally, the meteorological data for all identified land-breeze events at each individual tower location were archived (see Table 2.2 for quantities archived). To determine which towers experienced a land-breeze passage, the program examined 5-minute time-series data at the analysis grid point nearest to each tower. If the algorithm identified at least a 20° shift in wind direction from onshore to offshore in a span of 10 minutes, in combination with a maintenance of offshore winds for at least 25 minutes, then the tower location was considered to have experienced a land-breeze frontal passage. These data were then composited to determine the typical behavior of land breezes during this 7-year climatology.

Table 2.2. A list of the data archived for each land-breeze event to create a composite for the land-breeze climatology.

Quantity	*Archive characteristics*
Date*	Year, month, and day
Start and stop times	Time in UTC
Percentage of towers experiencing the land-breeze event	Ratio of the number of towers experiencing a land-breeze passage to the total number of towers available for the grid analysis
Number of hourly TTS fog observations*	Number of fog reports out of a possible 14
6-ft and 54-ft temperatures	Time series of all tower locations that experienced a land-breeze passage, at ±60 min of the passage
6-ft dew point temperature and relative humidity	Time series of all tower locations that experienced a land-breeze passage, at ±60 min of the passage
Wind direction change (absolute value)	Time series of all tower locations that experienced a land-breeze passage, at ±60 min of the passage
Wind speed	Time series of all tower locations that experienced a land-breeze passage, at ±60 min of the passage

*These parameters are archived for both land breeze and non-land breeze days.

2.4 Development of Forecast Tools

Each land-breeze event identified by the objective algorithm was manually validated prior to developing the forecast tools. Events that were subjectively considered weak or subtle were removed from the objective climatology data base in order to focus on only the most substantial land breezes with sharp, domain-wide wind shifts. A subjective classification of the synoptic flow was performed on the remaining events by examining MSLP fields from the NCEP/NCAR reanalysis archive. The NCEP/NCAR reanalysis maps of MSLP were examined at 0000 UTC for each land-breeze day to discern both the large-scale flow and MSLP gradient across the Florida peninsula. All events were then categorized according to the large-scale flow, magnitude of the MSLP gradient, and occurrence/absence of a sea breeze during the previous afternoon. In addition to these parameters, the temperature contrasts as a function of time were examined from Orlando, across selected KSC/CCAFS towers, and out to buoy 41009, 20 nm offshore of Cape Canaveral. Based on the results of the climatology, ZT92, and ZT93, these parameters were considered as potential predictors of land-breeze occurrence, onset time, and movement.

3. Analysis of Sample Land-Breeze Events

This section presents analyses of five sample land-breeze events from March to May 2000.

- 6 March: This case consisted of a very distinct, sharp land-breeze front between 0500–0600 UTC, accompanied by seasonal temperatures without a sea breeze the previous afternoon.
- 6 April: This night had unusually cold temperatures for this time of year and an extremely shallow land breeze late at night.
- 7 April: The temperatures increased from the previous night, and another much deeper land breeze occurred earlier during the night. Neither of these April events were accompanied by a sea breeze the previous afternoon.
- 27 April: This land breeze had an exceptionally deep circulation compared to the first three cases, and occurred after a sea breeze the previous afternoon.
- 12 May: This land breeze occurred after a sea breeze the previous afternoon and had the hottest surface temperatures of any of these events.

These sample events demonstrate the wide range of atmospheric characteristics associated with land breezes, and how different meteorological factors may lead to similar surface wind features found in the land-breeze frontal passages. In each of these events, it appears that the propagation rate of the land breeze is proportional to and bounded by the maximum wind speed observed at the 492-ft tall Tower 313.

3.1 6 March 2000 Event Without Sea Breeze

On the night of 6 March 2000, weak high pressure dominated the southeastern U.S. and the Florida peninsula (Fig. 3.1). The prevailing surface wind flow was light from the northeast (NE) and the skies were mostly clear with only patchy high clouds (not shown), creating ideal conditions for the development of a land breeze. A sharp land-breeze boundary developed and propagated eastward across KSC/CCAFS between 0500–0600 UTC. During the afternoon preceding the land breeze, the high temperature at Orlando, FL (MCO) was 78°F (26°C) with a low temperature of 53°F (12°C) during the night of the land breeze.

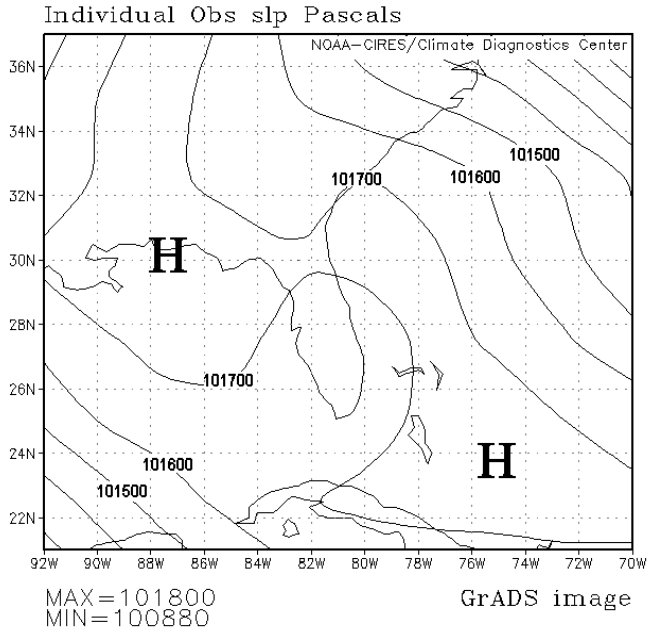

Figure 3.1. NCEP/NCAR reanalysis map of mean sea-level pressure over the southeastern U.S. at 0000 UTC 6 March 2000. The contour interval is 100 Pa (1 mb) with the maximum and minimum values indicated in the lower left.

The land breeze reached the westernmost KSC/CCAFS towers just before 0500 UTC and moved east of these towers by 0515 UTC (Fig. 3.2a). The land-breeze front quickly progressed eastward during the next 45 minutes, reaching western Merritt Island by 0530 UTC (Fig. 3.2b), eastern Merritt Island by 0545 UTC (Fig. 3.2c), and the tip of Cape Canaveral by 0600 UTC (Fig. 3.2d). The land breeze moved across the entire KSC/CCAFS tower network in just 1.4 hours. The time series plots of wind direction at the KSC/CCAFS Towers 1, 3, 506, and 1204 all exhibit a distinct wind shift from onshore to offshore between 0500 and 0600 UTC (Fig. 3.3a). The post land-breeze wind direction was initially from the west (W), but gradually veered to the northwest (NW) during the remainder of the night.

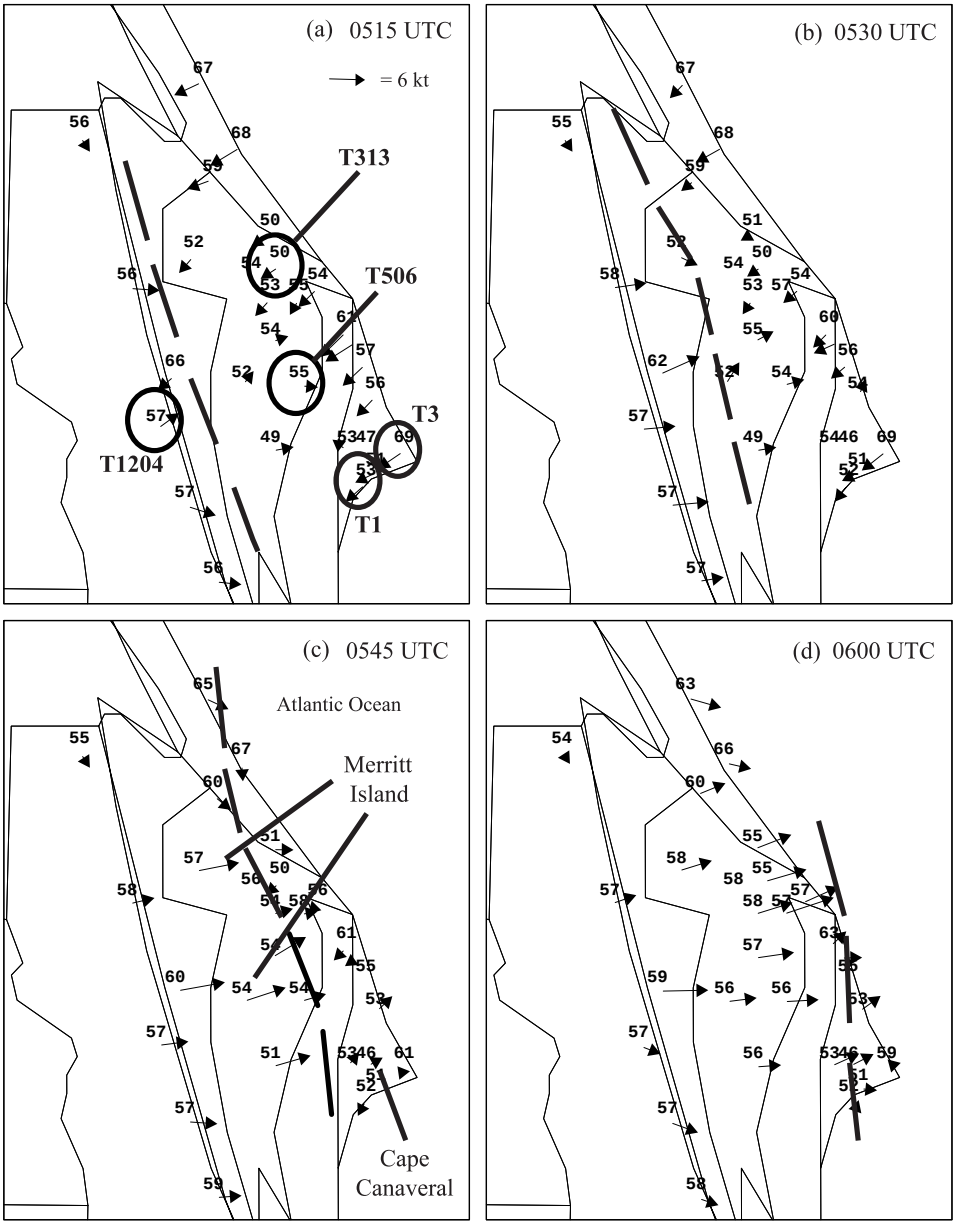

Figure 3.2. KSC/CCAFS tower observations of winds and 6-ft temperatures for 6 March 2000, valid at (a) 0515 UTC, (b) 0530 UTC, (c) 0545 UTC, and (d) 0600 UTC. The winds are given by arrows, with the tail centered on each station [speed scale provided in panel (a)], and 6-ft temperatures are plotted above the wind arrows. The locations of towers 1, 3, 313, 506, and 1204 for subsequent figures are circled in (a) and major geographical features are given in (c). Thick dashed lines denote the location of the land-breeze front.

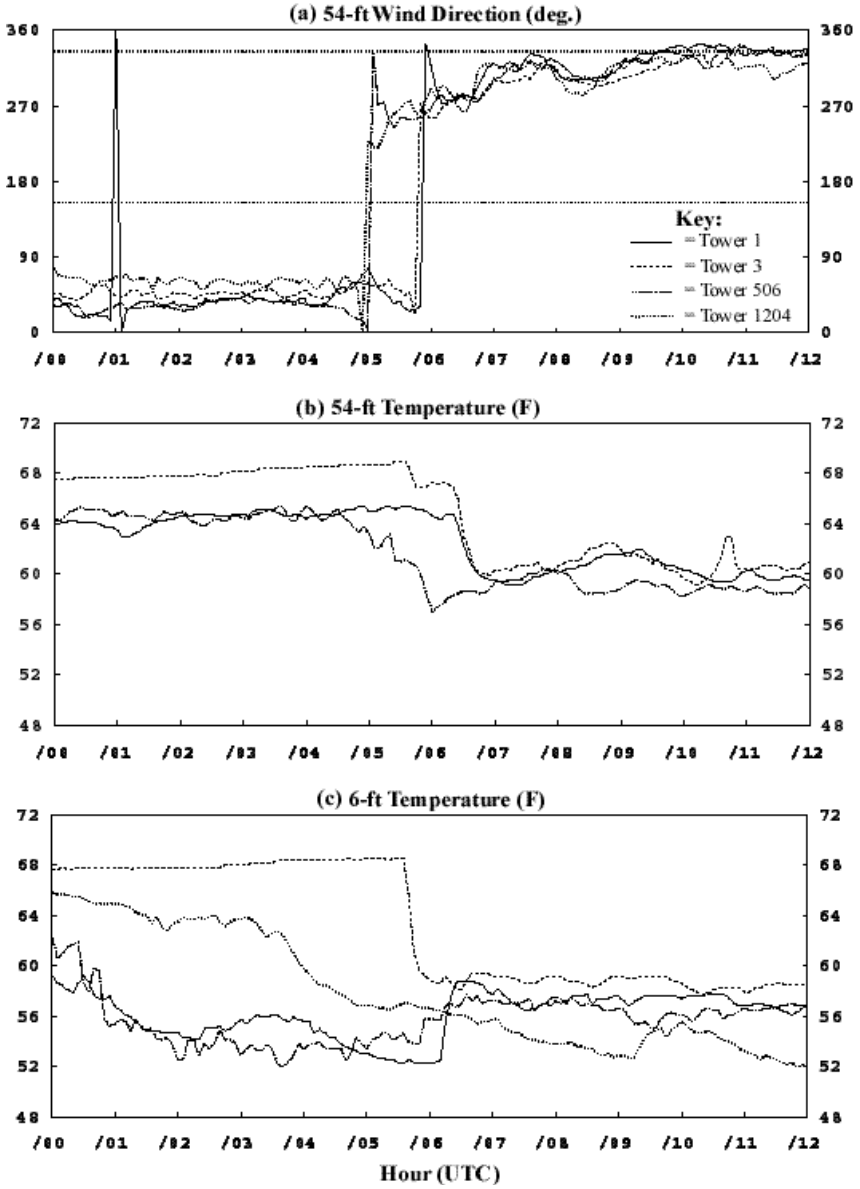

Figure 3.3. Time series plots for KSC/CCAFS Towers 1, 3, 506, and 1204, from 0000 to 1200 UTC 6 March 2000. Variables plotted are (a) 54-ft wind direction, (b) 54-ft temperature, and (c) 6-ft temperature. Note that 54-ft temperatures are not available for Tower 1204. The horizontal dotted lines in panel (a) differentiate between onshore and offshore wind direction. The key is provided in panel (a) and tower locations are shown in Fig. 3.2a.

Similar to the sea breeze but much weaker, the land-breeze circulation is typically driven by the temperature (density) contrast between the ocean and the land. The cooler, denser air over the land advances seaward, forming the land breeze. Lagging the wind shift by up to one hour, all three time series indicated a decrease in 54-ft temperatures associated with the land-breeze passage (Fig. 3.3b). However, the 6-ft temperature changes were not as straightforward. In fact, many of the 6-ft temperatures over Merritt Island increased by several degrees following the passage of the land breeze, especially by 0600 UTC (see Fig. 3.2). In addition, the time series plots in Fig. 3.3c show 6-ft temperature increases at Towers 1 and 506 at about 0600 UTC.

It is interesting to note that although Towers 1 and 3 are very close to each other, they exhibited completely different 6-ft temperature changes following the passage of the land breeze. The light NE wind flow maintained warm temperatures along the immediate coast at Tower 3 prior to the land breeze. Once the land-breeze front passed Tower 3, the 6-ft temperature dropped rapidly by about 10°F in 15 minutes. Conversely at Tower 1, there is enough land upstream under light NE flow to allow for radiational cooling and the development of a temperature inversion prior to the land breeze. This resulted in a temperature increase once the stronger winds of the land breeze eroded the shallow temperature inversion.

The vertical structure of the land breeze in the lowest 500 ft is shown in Fig. 3.4, which depicts a time-height cross section at the 492-ft tall Tower 313 (refer to Fig. 3.2a for location). Light NE flow of about 5 kt prevailed at all levels of Tower 313 until about 0600 UTC. Just prior to 0600 UTC, an abrupt wind shift occurred at all levels with the strongest W winds found between 100 and 200 ft. Note that the W flow is much weaker and fleeting above 300 ft, suggesting that the land-breeze circulation is not much deeper than 300 ft. The depth of the W flow is approximately an order of magnitude less than the observed depth of easterly low-level flow associated with the sea-breeze circulation over east-central Florida, consistent with ZT92.

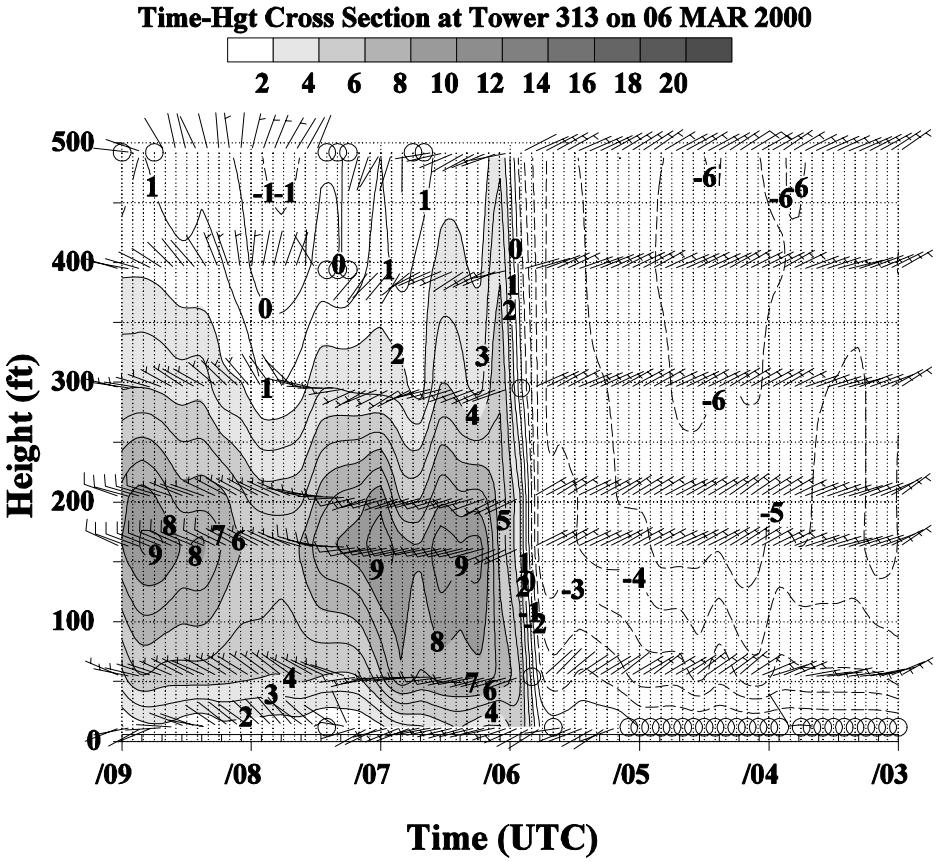

Figure 3.4. Time-height cross section of wind vectors and contoured u-wind component at Tower 313 from 0300–0900 UTC 6 March 2000. Time along the x-axis increases from right to left and height along the y-axis is given in feet. The u-wind component is contoured in 1-kt increments, with positive (westerly) u-winds greater than 2 kt shaded according to the scale provided.

3.2 6 April 2000 Event Without Sea Breeze

On 6 April 2000, a large area of high pressure stretched from the northeastern Gulf of Mexico across the Florida peninsula into the western Atlantic (Fig. 3.5). The surface flow was light and variable beneath the high pressure ridge over east-central Florida. In addition, temperatures were unseasonably cold for this time of year.

The high temperature during the afternoon preceding the land breeze was only 69°F (21°C) at Melbourne, FL (MLB) and 72°F (22°C) at MCO, whereas the low temperature the night of the land breeze was 42°F (6°C) at MLB and 41°F (5°C) at MCO.

The land-breeze front on 6 April propagated much slower than the 6 March event and developed later at night. The land-breeze front moved into the northwestern portion of the KSC/CCAFS tower network by about 0830 UTC (Fig. 3.6a), accompanied by NW winds behind the front. The front moved to the southeast (SE) reaching northern Merritt Island by 0900 UTC (Fig. 3.6b) and central Merritt Island by 0930 UTC (Fig. 3.6c). The land-breeze front approached Cape Canaveral by 1000 UTC (Fig. 3.6d) and did not clear the KSC/CCAFS domain until well after 1000 UTC (not shown).

The 54-ft winds were generally light and variable prior to the land breeze and NW at about 6 to 8 kt after the land-breeze frontal passage. The 6-ft temperatures did not exhibit a significant change with the frontal passage except over northern Merritt Island. At these locations, the temperatures warmed by 6–10°F in one hour (e.g. from 0830 to 0930 UTC at the towers circled in Figs. 3.6a and c).

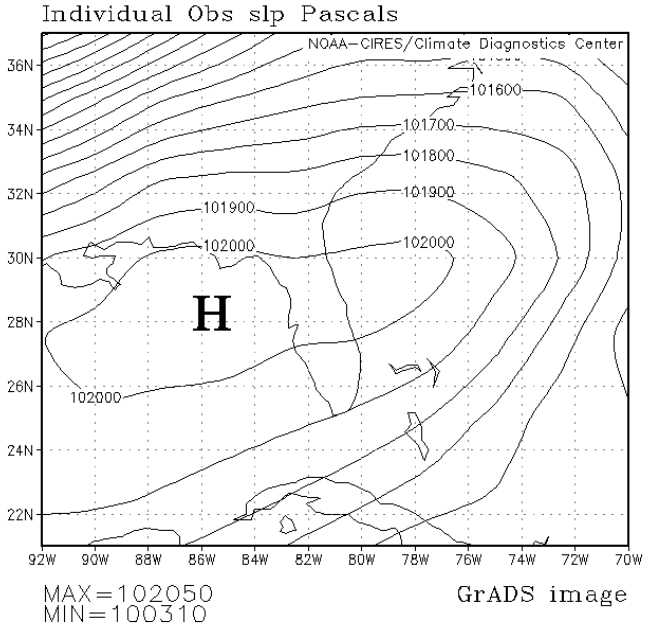

Figure 3.5. NCEP/NCAR reanalysis map of mean sea-level pressure over the southeastern U.S. at 0000 UTC 6 April 2000. The contour interval is 100 Pa (1 mb) with the maximum and minimum values indicated in the lower left.

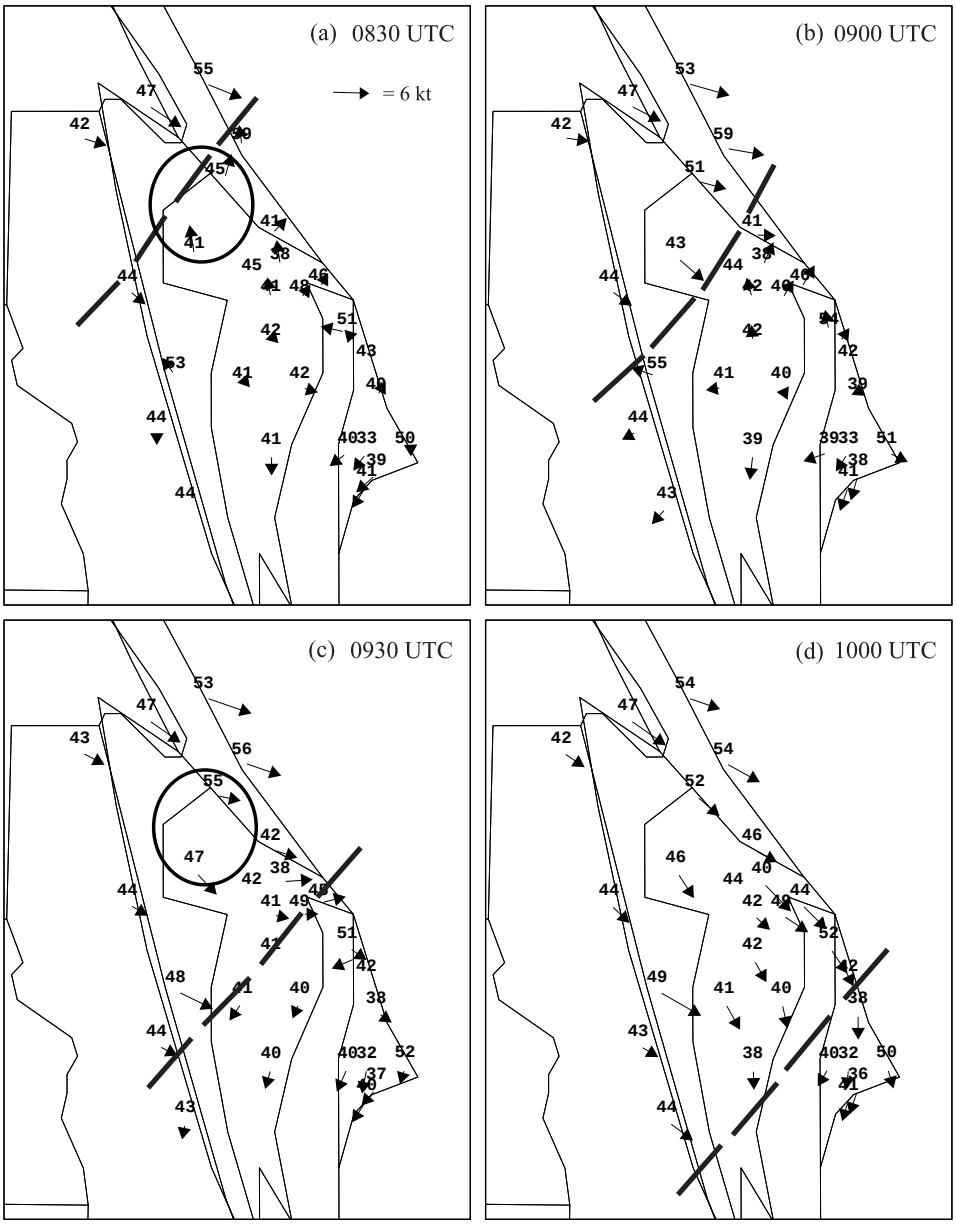

Figure 3.6. KSC/CCAFS tower observations of winds and 6-ft temperatures for 6 April 2000, valid at (a) 0830 UTC, (b) 0900 UTC, (c) 0930 UTC, and (d) 1000 UTC. The winds are given by arrows, with the tail centered on each station [speed scale provided in panel (a)], and 6-ft temperatures are plotted above the wind arrows. Thick dashed lines denote the location of the land-breeze front. The circled towers are discussed in the text.

The time-height cross section at Tower 313 (Fig. 3.7) shows the very shallow nature of this land-breeze event. Prior to the land breeze, the winds were light from the SE until 0930 UTC. After 0930 UTC, the winds shifted to NW from the surface up to about 250 ft while the winds above 250 ft shifted to a north (N) to NE direction. The W wind component continued below 250 ft until about 1245 UTC, whereas above 250 ft the winds shifted back to light SE after 1130 UTC. Also, the slower propagation rate of this event is directly related to the lower peak wind speed at Tower 313 (~5kt at 150 ft, Fig. 3.7) compared to the 6 March case (~9–10 kt at 150 ft, Fig. 3.4).

Since the land-breeze circulation was so shallow on this night, it barely showed any signal in the 915-MHz DRWP time-height cross section at profiler #3 (central Merritt Island location, see Fig. 2.1). There is evidence of a subtle shift from E to NE winds below 1000 ft between 0900 and 1100 UTC (Fig. 3.8), but the transition was quite smooth. Above 1000 ft, there is no indication of any substantial wind shift related to a surface-based land breeze. Overall, the 915-MHz DRWP time-height cross section does not indicate any W flow associated with the land-breeze circulation.

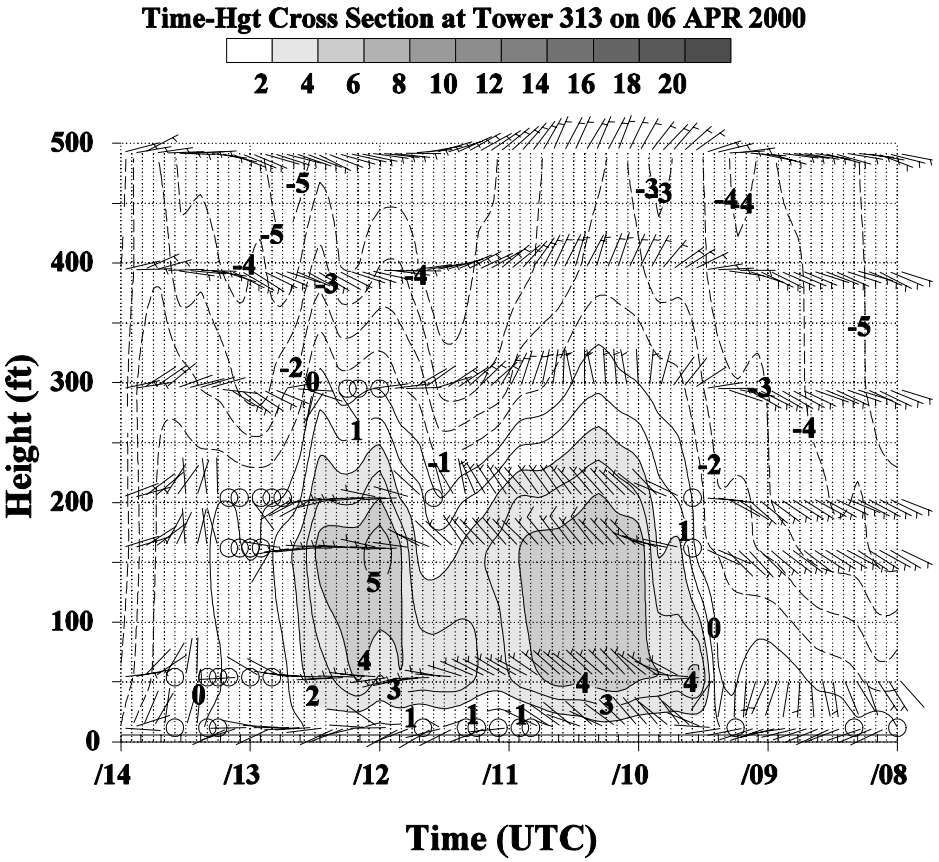

Figure 3.7. Time-height cross section of wind vectors and contoured u-wind component at Tower 313 from 0800 to 1400 UTC 6 April 2000. Time along the x-axis increases from right to left and height along the y-axis is given in feet. The u-wind component is contoured in 1-kt increments, with positive (westerly) u-winds greater than 2 kt shaded according to the scale provided.

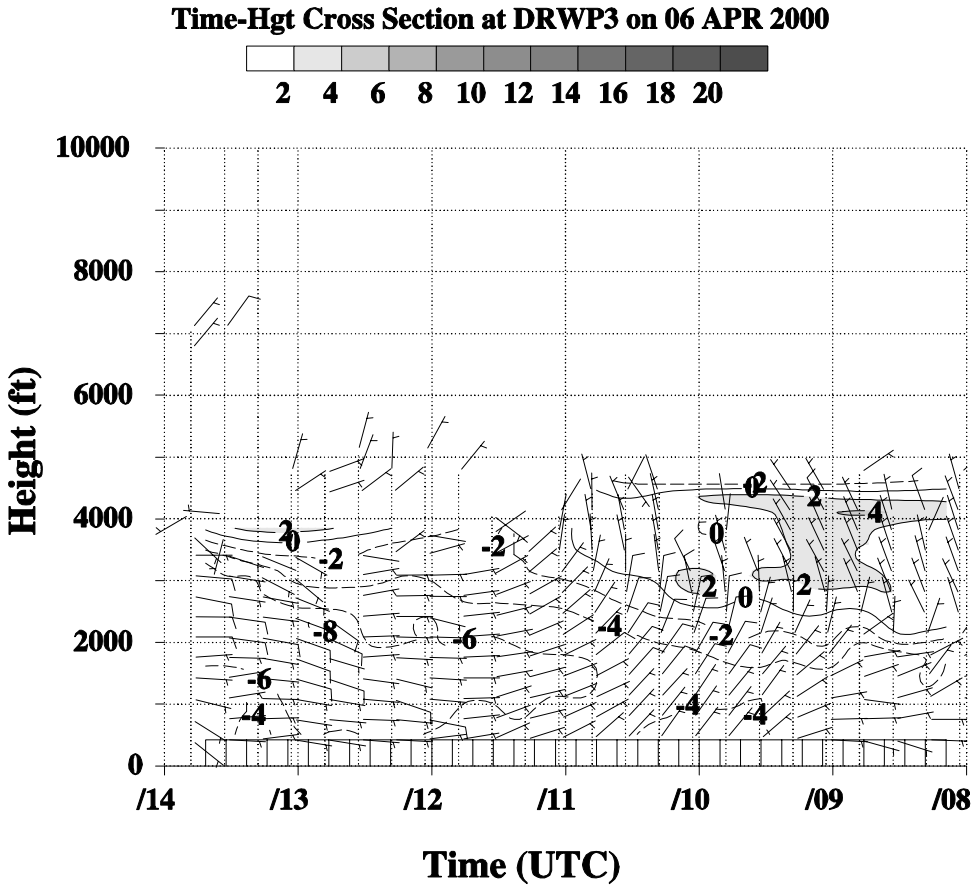

Figure 3.8. Time-height cross section of wind vectors and contoured u-wind component at the 915-MHz DRWP #3 from 0800 to 1400 UTC 6 April 2000. Time along the x-axis increases from right to left and height along the y-axis is given in feet. The u-wind component is contoured in 2-kt increments, with positive (westerly) u-winds greater than 2 kt shaded according to the scale provided.

3.3 7 April 2000 Event Without Sea Breeze

The land-breeze passage on the night of 7 April was much deeper and sharper than the previous night's land breeze. The synoptic conditions were again favorable for land-breeze formation since surface high pressure still dominated the Florida peninsula and the prevailing winds were sufficiently light. The area of high pressure moved eastward into the western Atlantic with a ridge axis centered just south of KSC/CCAFS (Fig. 3.9). As a result, the large-scale wind flow was from the south (S) during the night. The high temperature at MCO during the previous afternoon was 79°F (26°C) with a low temperature of 52°F (11°C) during the night of the land breeze.

The land breeze began in the KSC/CCAFS domain by 0500 UTC and propagated through the tower network in about 1.5 to 2 hours. At 0500 UTC, the land-breeze front was oriented southwest (SW) to NE and was situated over the northwestern portion of the tower network (Fig. 3.10a). The front moved to the SE into northwestern Merritt Island by 0530 UTC (Fig. 3.10b), with W winds behind the front at a slightly higher speed than the S winds ahead of the front. The front continued its southeastward progress over the next hour, reaching eastern Merritt Island by 0600 UTC (Fig. 3.10c), and Cape Canaveral and southern Merritt Island by 0630 UTC (Fig. 3.10d). During these times, the post-frontal winds backed slightly to a W-SW direction.

At most stations, the 6-ft temperatures remained nearly the same following the passage of the land-breeze front; however, many stations that had onshore flow prior to the land breeze experienced a decrease in the 6-ft temperatures after frontal passage. The towers along the immediate Atlantic coast had a temperature decrease as large as 9°F in one hour (Fig. 3.10).

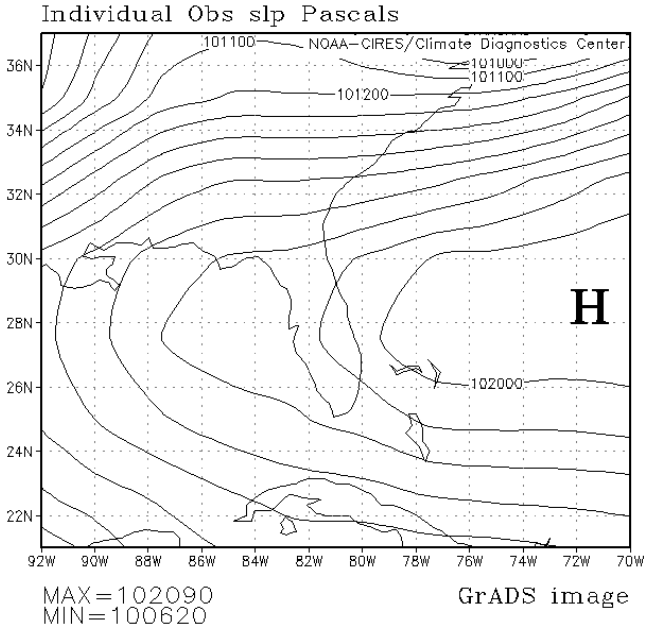

Figure 3.9. NCEP/NCAR reanalysis map of mean sea-level pressure over the southeastern U.S. at 0000 UTC 7 April 2000. The contour interval is 100 Pa (1 mb) with the maximum and minimum values indicated in the lower left.

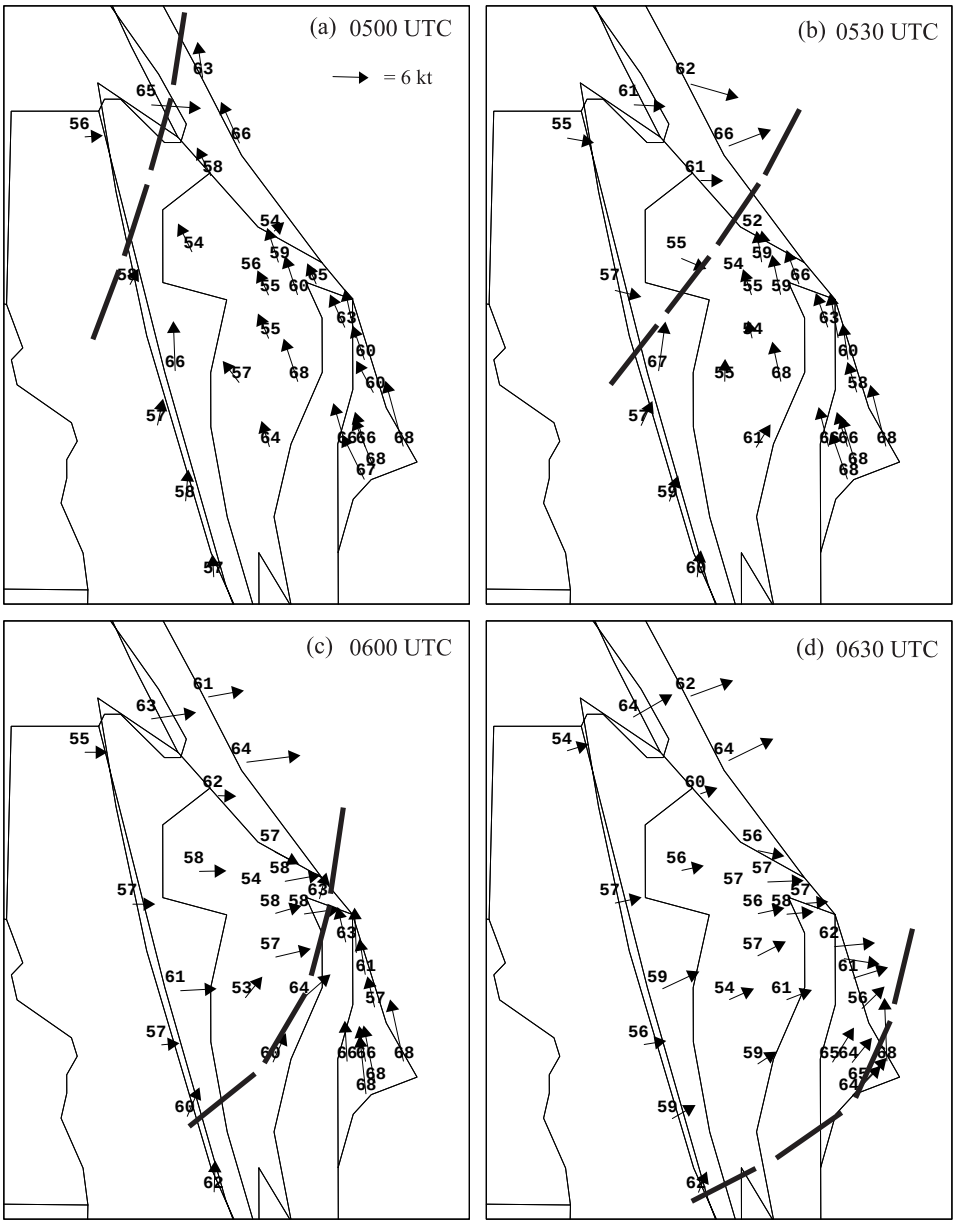

Figure 3.10. KSC/CCAFS tower observations of winds and 6-ft temperatures for 7 April 2000, valid at (a) 0500 UTC, (b) 0530 UTC, (c) 0600 UTC, and (d) 0630 UTC. The winds are given by arrows, with the tail centered on each station [speed scale provided in panel (a)], and 6-ft temperatures are plotted above the wind arrows. Thick dashed lines denote the location of the land-breeze front.

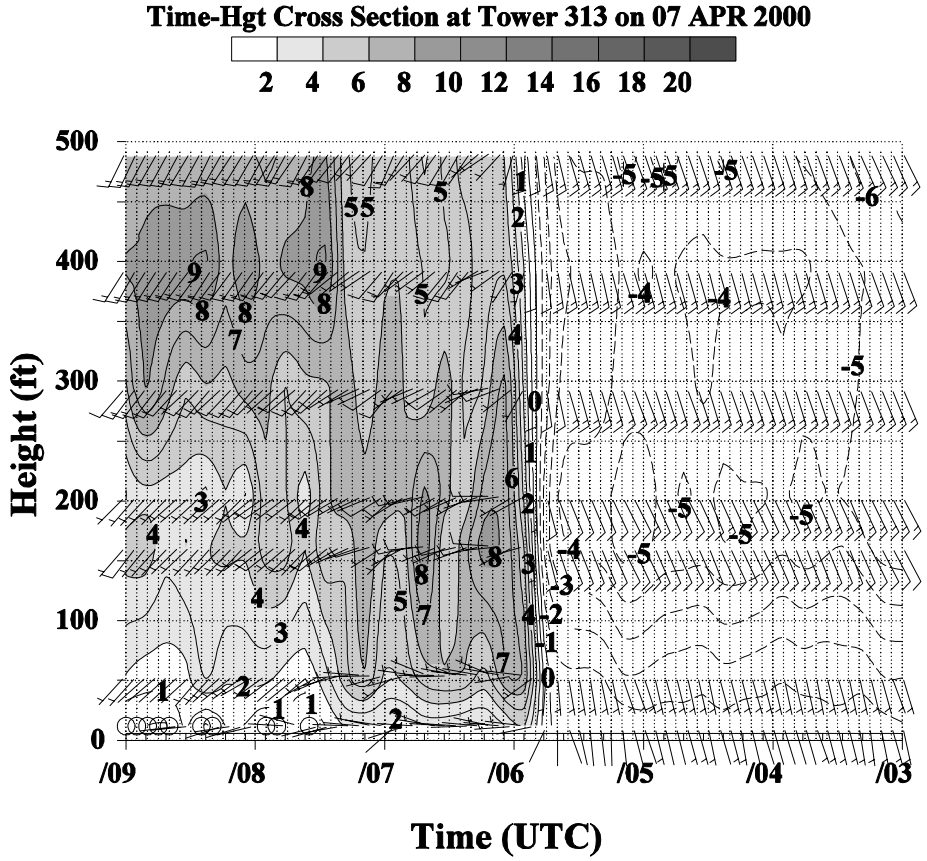

Figure 3.11. Time-height cross section of wind vectors and contoured u-wind component at Tower 313 from 0300 to 0900 UTC 7 April 2000. Time along the x-axis increases from right to left and height along the y-axis is given in feet. The u-wind component is contoured in 1-kt increments, with positive (westerly) u-winds greater than 2 kt shaded according to the scale provided.

The time-height cross section at Tower 313 indicates that the 7 April land breeze was quite deep. South to southeasterly flow prevailed at all levels prior to the land-breeze onset whereas SW flow occurred after the land-breeze passage (Fig. 3.11). The vertical profile of the wind shift was steeply sloped with the shift to W winds occurring just before 0600 UTC near the surface, and just after 0600 UTC at 500 ft. The 7 April land-breeze circulation was much stronger than the 6 April event since the maximum magnitude of the positive u-wind component (8–9 kt, Fig. 3.11) is nearly double that of the previous night (4–5 kt, Fig 3.7).

The land breeze on 7 April is evident in the lowest gates of the 915-MHz DRWP over central Merritt Island, shown in Fig. 3.12. Southeasterly flow prevailed up to 2000 ft prior to the land-breeze passage and a slight wind shift occurred just before 0600 UTC. The westerly u-wind components (shading in Fig. 3.12) associated with the land breeze were found up to 1000 ft or so between 0600 and 0900 UTC.

Based on the 915-MHz DRWP cross section, there is little indication of a landward-directed return current above the land breeze, as is typically found in a sea-breeze circulation. Instead, the winds gradually became S above 2000 ft, and turned to SW between 3000–4000 ft. The W winds at about 3000 ft were prevalent prior to the initiation of the low-level land breeze. Above this band of westerlies, weak E winds developed by 0700 UTC, but these winds are not considered a return current since they were substantially separated from the westerly u-winds associated with the surface-based land breeze.

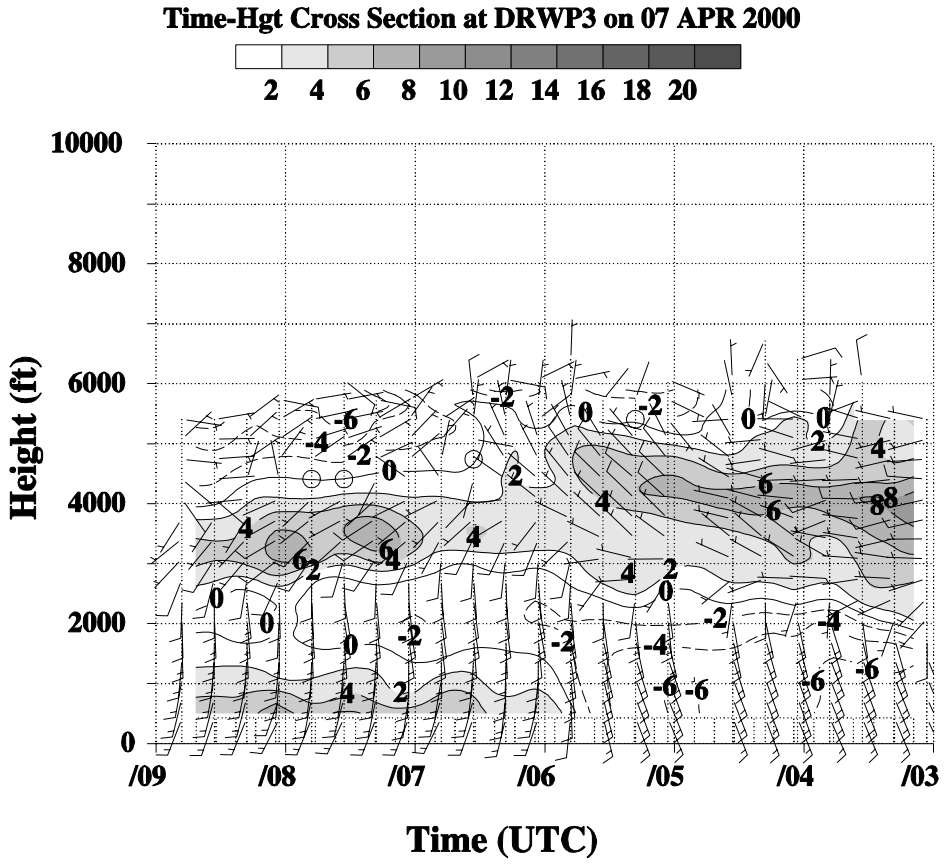

Figure 3.12. Time-height cross section of wind vectors and contoured u-wind component at the 915-MHz DRWP #3 from 0300 to 0900 UTC 7 April 2000. Time along the x-axis increases from right to left and height along the y-axis is given in feet. The u-wind component is contoured in 2-kt increments, with positive (westerly) u-winds greater than 2 kt shaded according to the scale provided.

3.4 27 April 2000 Event With Sea Breeze

The land breezes discussed in the previous sections developed without the occurrence of a sea breeze during the preceding afternoon. The 27 April land breeze, however, had a sea-breeze circulation develop and move onshore initially at about 1600 UTC the previous afternoon. MCO had a high temperature of 79°F (26°C) the afternoon preceding the land breeze and a low temperature of 55°F (13°C) during the night of the land breeze. This land-breeze event was most likely the sea-breeze convergence boundary "retreating" eastward as the circulation cell weakened and collapsed after sunset. The early onset time of this land breeze also suggests that it was a retreating sea breeze rather than a thermally-driven nocturnal circulation.

The surface synoptic flow was as light as the previous events discussed. A broad, weak trough of low pressure was located well offshore of the Florida east coast at 0000 UTC, with another trough to the north of Florida (Fig. 3.13). A weak area of high pressure was situated over the Gulf of Mexico providing a light N large-scale flow across the Florida peninsula.

The land breeze was preceded by NE winds associated with the sea-breeze circulation that developed the previous afternoon. At 0230 UTC, the land-breeze front was over mainland Florida, in the western edge of the network (Fig. 3.14a). The front moved quickly eastward reaching central Merritt Island by 0300 UTC and Cape Canaveral by 0330 UTC (Figs. 3.14b-c). The land-breeze front cleared the coast by 0400 UTC and W-NW winds prevailed across the entire KSC/CCAFS tower network following the front (Fig. 3.14d).

The 6-ft temperature changes associated with the land breeze were most pronounced at the coastal tower locations. Temperatures along the coast generally ranged from the high 60s to low 70s prior to the land-breeze frontal passage (Figs. 3.14a-b), and then dropped to the low to mid 60s afterwards (Figs. 3.14c-d). A few stations experienced a slight temperature increase with the land breeze, particularly those locations that did not have onshore winds directly adjacent to a water body. In those instances, the increased wind speeds associated with the land breeze mix the atmosphere sufficiently to break the surface temperature inversion, resulting in increased surface temperatures.

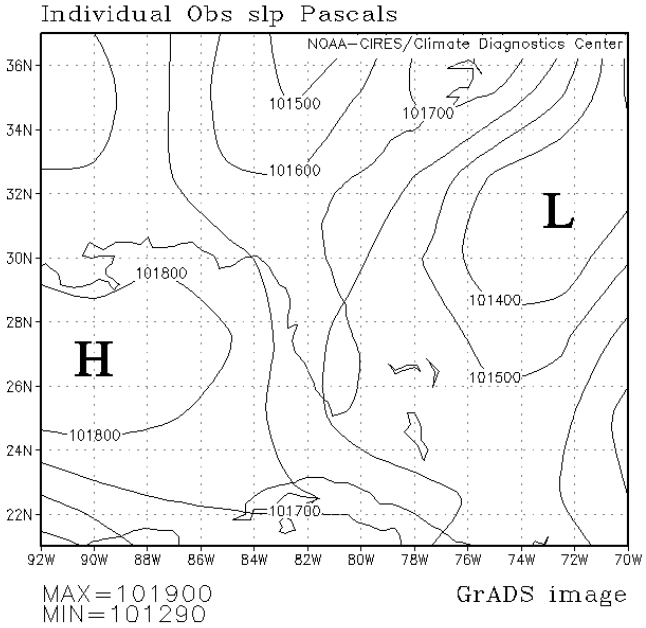

Figure 3.13. NCEP/NCAR reanalysis map of mean sea-level pressure over the southeastern U.S. at 0000 UTC 27 April 2000. The contour interval is 100 Pa (1 mb) with the maximum and minimum values indicated in the lower left.

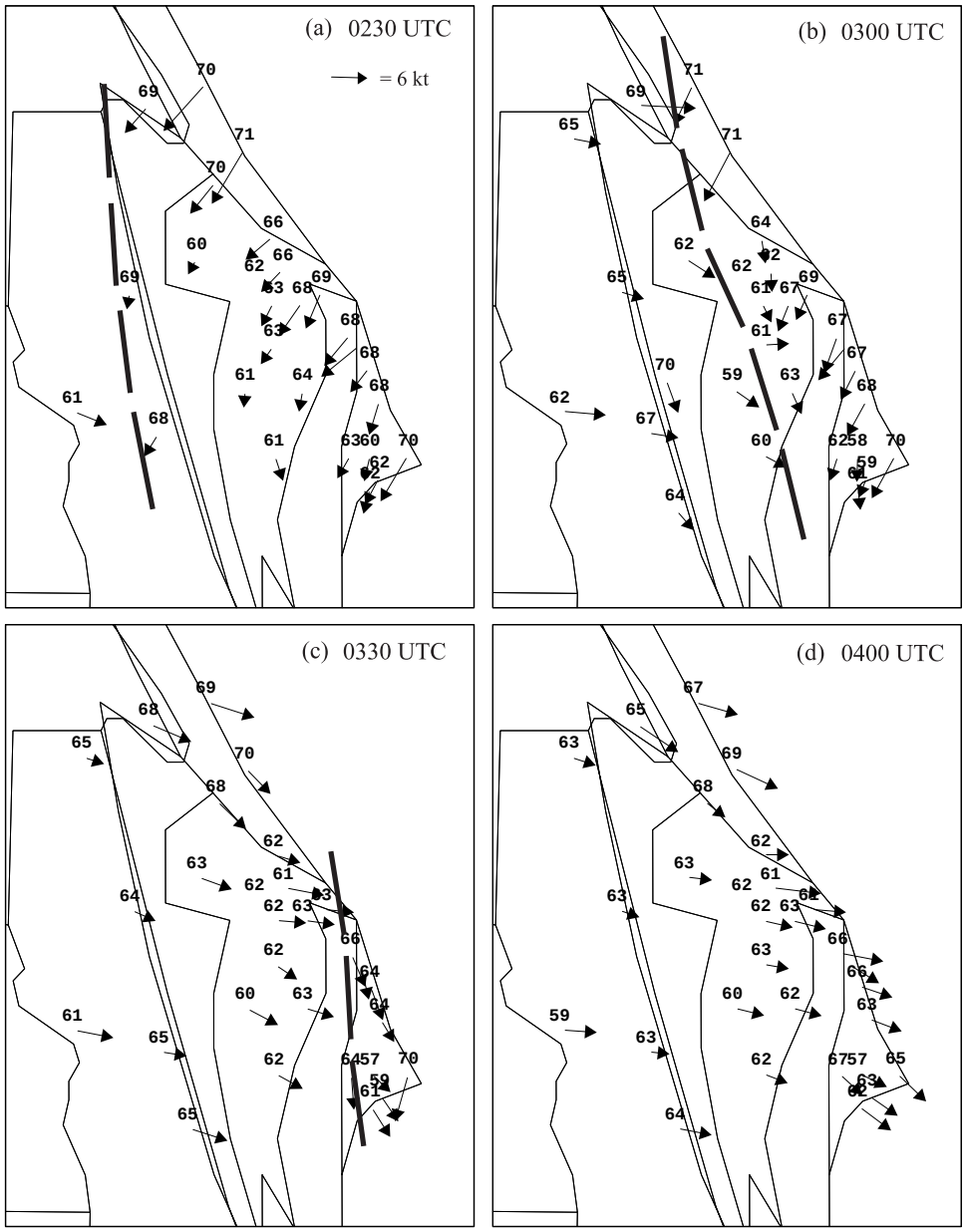

Figure 3.14. KSC/CCAFS tower observations of winds and 6-ft temperatures for 27 April 2000, valid at (a) 0230 UTC, (b) 0300 UTC, (c) 0330 UTC, and (d) 0400 UTC. The winds are given by arrows, with the tail centered on each station [speed scale provided in panel (a)], and 6-ft temperatures are plotted above the wind arrows. Thick dashed lines denote the location of the land-breeze front.

The time-height cross section at Tower 313 shows a dramatic shift from onshore to offshore winds as the land-breeze front moves through at 0300 UTC (Fig. 3.15). The maximum u-wind component reached 12 kt at 200 ft between 0400 and 0500 UTC. The sharp wind shift occurred at all levels of Tower 313 in a short time period, indicating a steep slope to this land-breeze front.

The 915-MHz DRWP #3 provided evidence that the depth of the offshore winds was over 1500 ft. In Fig. 3.16, a wind shift from NE to NW was evident shortly after 0300 UTC up to 1500 ft. The NW winds deepened with time and eventually eroded all E winds associated with the collapsing sea-breeze circulation cell by 0430 UTC. By 0600 UTC, W-NW winds occurred from the surface to 10000 ft. This case was representative of many land-breeze events that replaced the daytime sea-breeze circulation. Distinct, sharp wind-shift lines often accompanied the "retreating sea breeze" with the depth of the vertical circulation comparable to that of the sea breeze.

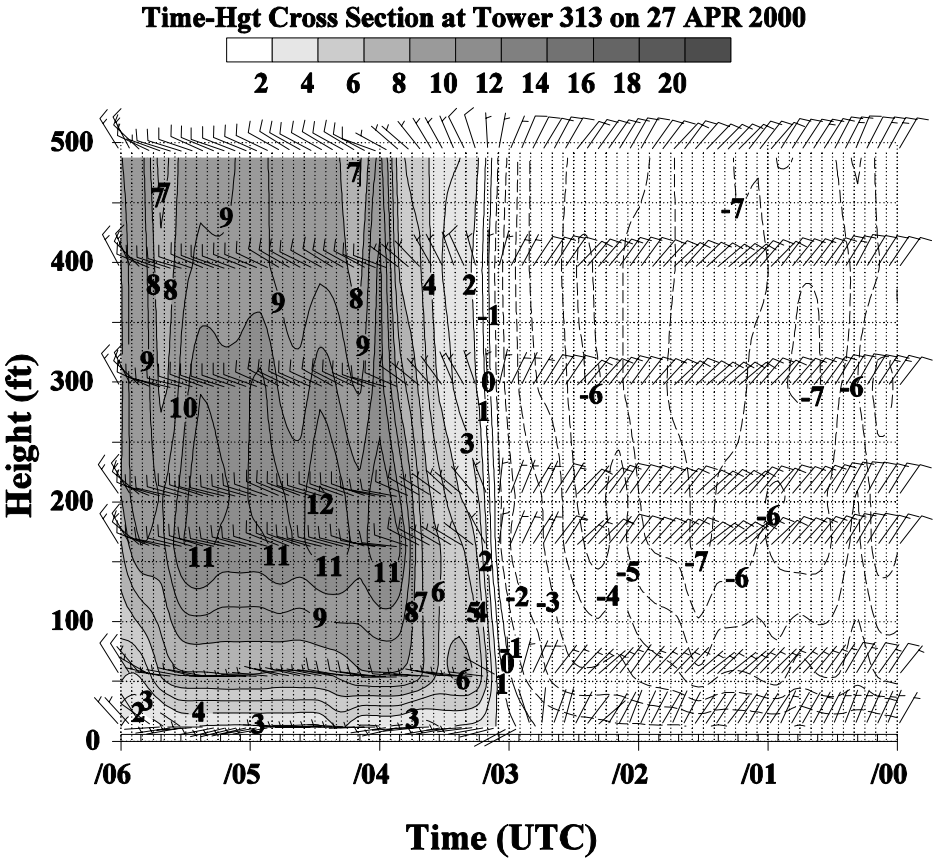

Figure 3.15. Time-height cross section of wind vectors and contoured u-wind component at Tower 313 from 0000 to 0600 UTC 27 April 2000. Time along the x-axis increases from right to left and height along the y-axis is given in feet. The u-wind component is contoured in 1-kt increments, with positive (westerly) u-winds greater than 2 kt shaded according to the scale provided.

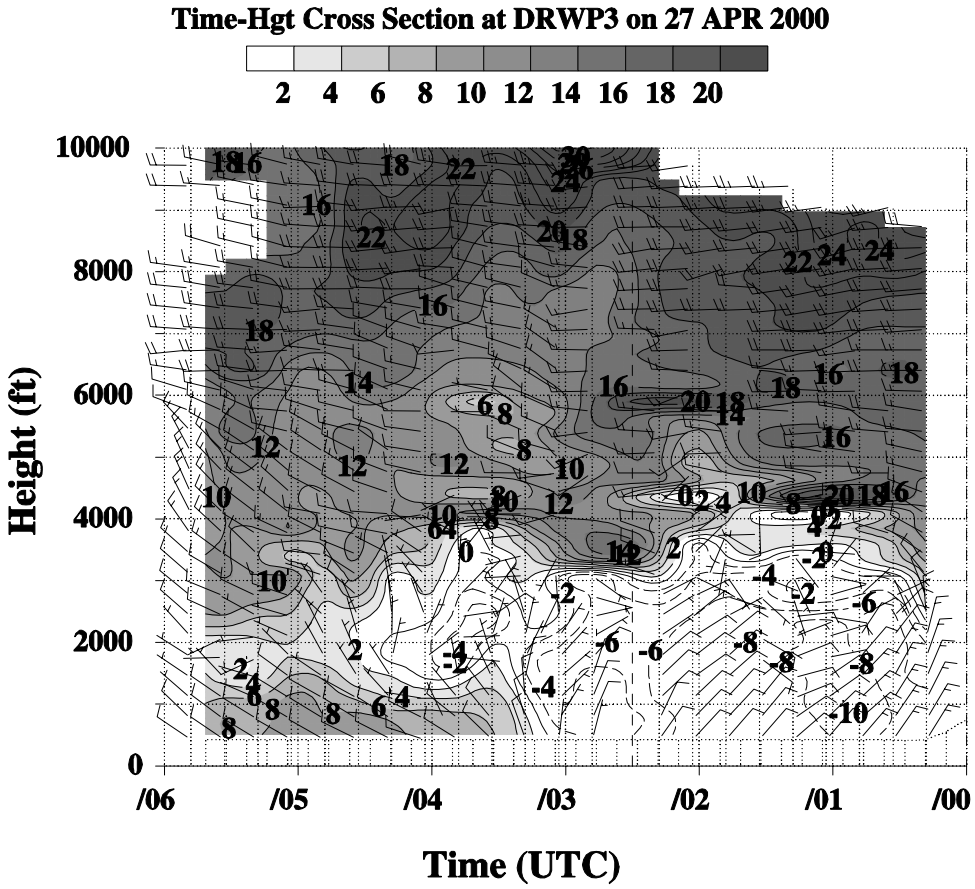

Figure 3.16. Time-height cross section of wind vectors and contoured u-wind component at the 915-MHz DRWP #3 from 0000 to 0600 UTC 27 April 2000. Time along the x-axis increases from right to left and height along the y-axis is given in feet. The u-wind component is contoured in 2-kt increments, with positive (westerly) u-winds greater than 2 kt shaded according to the scale provided.

3.5 12 May 2000 Event With Sea Breeze

The 12 May land breeze also followed a sea breeze from the previous afternoon, behaving much like a retreating sea-breeze boundary during the collapse of the circulation; however, the 12 May event occurred in two separate surges. The first surge, accompanied by SW winds, appeared to be the retreating sea-breeze front, which was later reinforced by a surge from the NW. Time-height cross sections at Tower 313 and the 915-MHz DRWP #3 over central Merritt Island illustrate the vertical structure of the land breeze, as well as to demonstrate the modulation of the inertial oscillation by the land- and sea-breeze circulations (which results in a 360° clockwise turning of the wind direction in about one day).

The synoptic flow at the surface on 12 May was similar to the previous events described. At 0000 UTC, a high pressure ridge was situated over the Bahamas extending across the Florida peninsula into the Gulf of Mexico (Fig. 3.17). The prevailing large-scale flow was from the SW across east-central Florida at 0000 UTC. The temperatures on 11–12 May were warmer than the previous events described. The afternoon high temperature at MCO was 93°F (34°C) while the low temperature was 66°F (19°C) during the night of the land breeze.

South to southeast wind flow prevailed at 54 ft prior to the land-breeze passage (Fig. 3.18a). By 0330 UTC, the land-breeze front had entered the KSC/CCAFS observational network extending from northern Merritt Island, southwestward to Mainland Florida. The leading edge of the land breeze propagated steadily to the E–SE over the next hour reaching the tip of Cape Canaveral by 0430 UTC (Figs. 3.18c-d). Light W winds of 6 kt or less occurred behind the land-breeze front. The post-frontal wind direction backed from W to SW between 0330 and 0430 UTC while the speeds decreased (Figs. 3.18b-d).

The cooling at 6 ft associated with the land breeze was minimal with the passage of the front. At most stations, the temperatures remained nearly the same, but a few stations in the northern portion of KSC/CCAFS cooled by 2°F in one hour. After land-breeze passage, the temperatures at most stations were still in the mid to upper 70s.

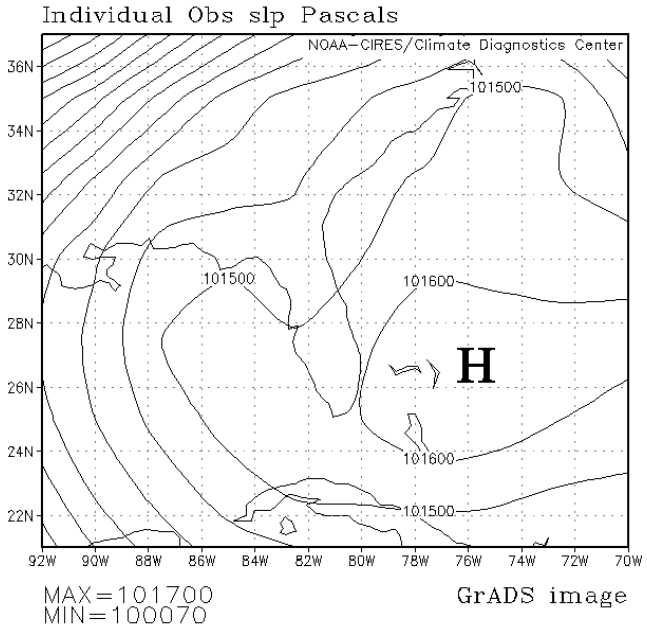

Figure 3.17. NCEP/NCAR reanalysis map of mean sea-level pressure over the southeastern U.S. at 0000 UTC 12 May 2000. The contour interval is 100 Pa (1 mb) with the maximum and minimum values indicated in the lower left.

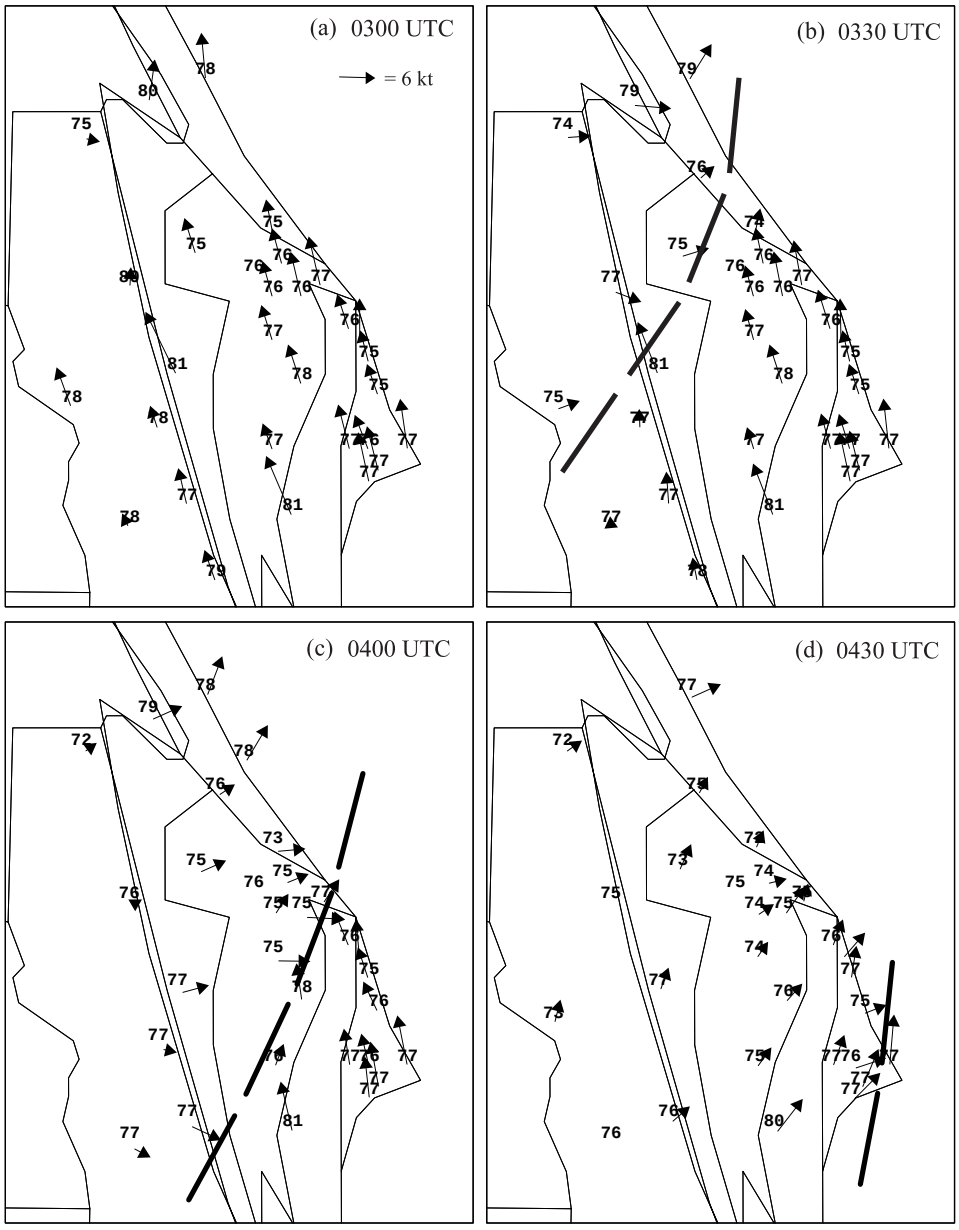

Figure 3.18. KSC/CCAFS tower observations of winds and 6-ft temperatures for 12 May 2000, valid at (a) 0300 UTC, (b) 0330 UTC, (c) 0400 UTC, and (d) 0430 UTC. The winds are given by arrows, with the tail centered on each station [speed scale provided in panel (a)], and 6-ft temperatures are plotted above the wind arrows. Thick dashed lines denote the location of the land-breeze front.

The time-height cross section at Tower 313 clearly depicts the land-breeze passage at 0400 UTC (Fig. 3.19a). The wind shift from SE to SW was most distinct below 300 ft, but was evident at all levels. It appears that the initial surge between 0400 and 0500 UTC was strongest, with wind speeds weakening after 0500 UTC. The SW flow strengthened again at all levels after 0600 UTC, with a peak value of 8 kt at 400 ft and 0730 UTC (Fig. 3.19b). The second surge occurred at 0900 UTC, accompanied by a directional shift to the NW and an increase in wind speeds at all levels of Tower 313.

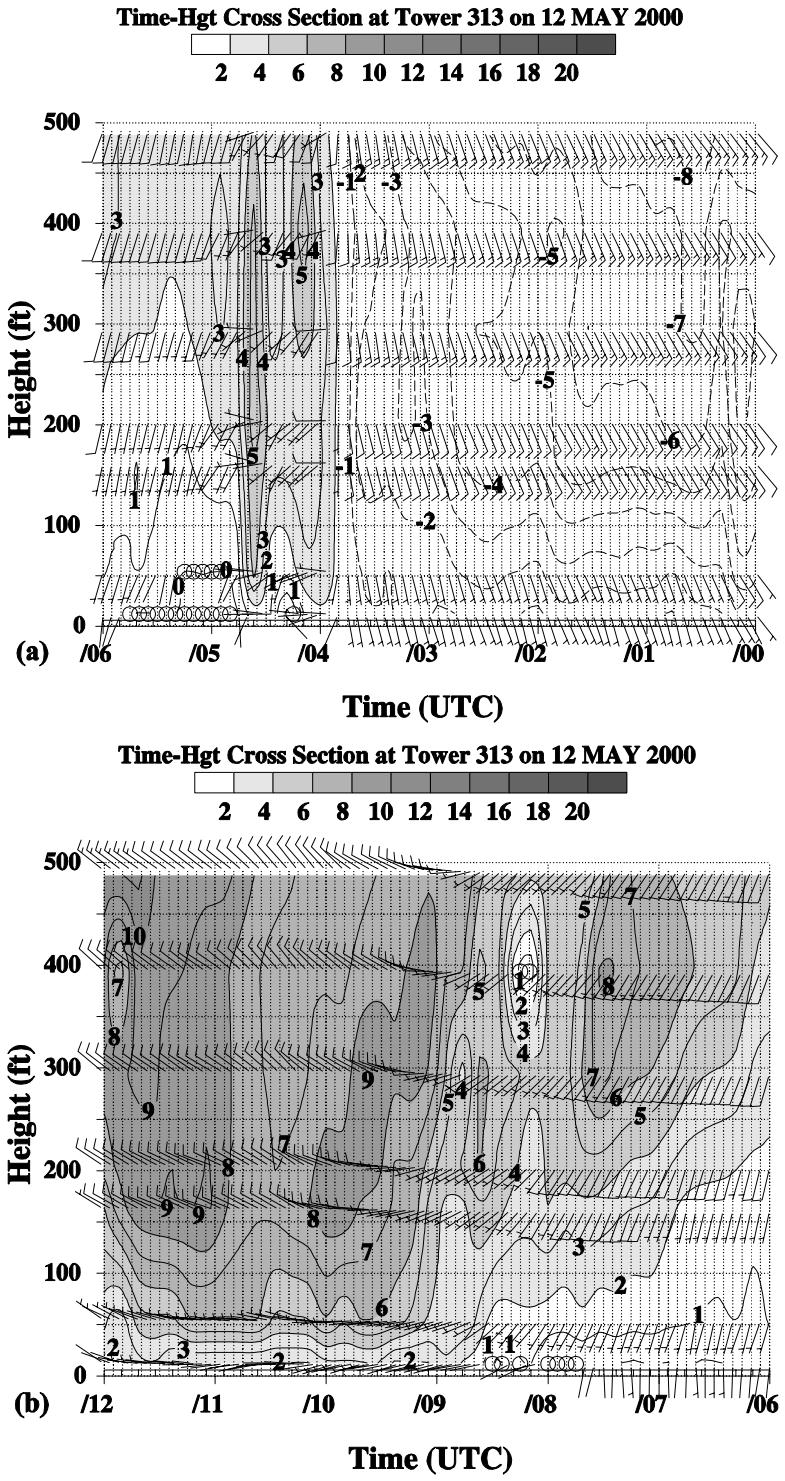

Figure 3.19. Time-height cross section of wind vectors and contoured u-wind component at Tower 313 on 12 May 2000 from (a) 0000 to 0600 UTC, and (b) 0600 to 1200 UTC. Time along the x-axis increases from right to left and height along the y-axis is given in feet. The u-wind component is contoured in 1-kt increments, with positive (westerly) u-winds greater than 2 kt shaded according to the scale provided.

The 915-MHz DRWP #3 shows both surges in the land breeze quite well (Fig. 3.20). The initial directional shift to the SW occurred between 0400 and 0500 UTC up to a height of 3000 ft (Fig. 3.20a). A southerly low-level jet of about 30 kt developed between 1500 and 3000 ft, nearly coincident with the passage of the initial surge. Southwesterly flow prevailed up to 4000 ft following the land-breeze passage until 0900 UTC. At 0900 UTC, a shift to NW winds occurred in the lowest 2000 ft and remained until about 1400 UTC (Fig. 3.20b).

After 1400 UTC, the sea-breeze circulation began below 2000 ft, and continued to deepen over the next several hours. At the same time, the wind direction in the lowest 2000 ft continued to rotate clockwise, becoming SE once again by 1900 UTC. The onshore flow associated with the sea-breeze circulation deepened to about 4000 ft by 2300 UTC, and a well-developed W return flow developed aloft by 1900 UTC and continued throughout the rest of the day in the 5000- to 8000-ft layer.

The evolution of this wind flow as depicted by the 915-MHz DRWP illustrates the inertial oscillation of the low-level wind field below 2000 ft, and its modulation by the land- and sea-breeze fronts. From 0000 UTC 12 May to 0000 UTC 13 May, the low-level wind direction experienced a complete 360° clockwise rotation with fairly uniform direction changes. The sharpest changes in wind direction occurred with the two land-breeze surges at 0400 and 0900 UTC, and with the onset of the sea breeze after 1400 UTC.

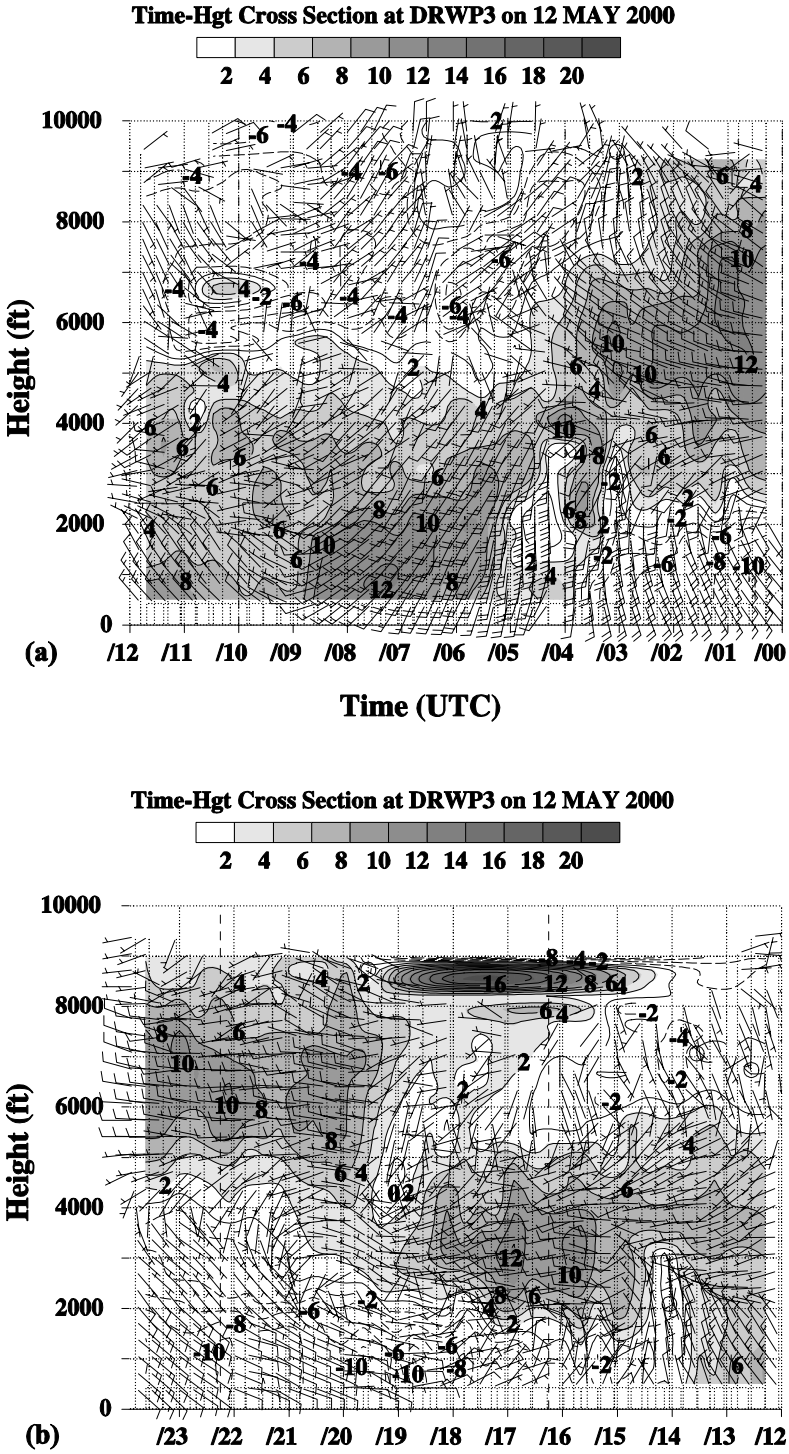

Figure 3.20. Time-height cross section of wind vectors and contoured u-wind component at the 915-MHz DRWP #3 on 12 May 2000 from (a) 0000 to 1200 UTC, and (b) 1200 to 2355 UTC. Time along the x-axis increases from right to left and height along the y-axis is given in feet. The u-wind component is contoured every 2 kt, with positive (westerly) u-winds greater than 2 kt shaded according to the scale provided.

4. Land-Breeze Climatology Results

This section provides a summary of the 7-year climatology of land-breeze events at the KSC/CCAFS towers from February 1995 to January 2002. The results focus on features and distributions of land breezes that helped shape the qualitative forecast tools presented in Section 5. The data were divided into Minimal Convective (MC, October to May) and Peak Convective months (PC, June to September), and categorized by weather regime in order to develop forecast guidance for determining the land-breeze occurrence, timing, and movement.

4.1 Summary of Events Classified by Program

The objective identification program described in Section 2.3 underestimated the total number of land-breeze events in the 1999 to 2000 test season [probability of detection (POD) of 68%] since it was designed to have a near zero FAR. However, the low POD for the developmental season could have been caused by frequent periods of missing data at several tower sites throughout the season. The subsequent analyses experienced periodic discontinuities and coverage gaps due to these missing data. As a result, some land-breeze events identified subjectively could not be classified objectively in the developmental season.

4.1.1 Monthly Occurrence

The algorithm identified 393 land-breeze events during the 7-year period, which were validated by a subjective examination of each identified event. The number of events for each month is shown in Table 4.1 along with the totals and averages for each month and year. The number of events in a given month varies significantly, ranging from 0 events in December 1997, September 1998, and October 2001 to 13 events in April 1999 and July 1999; however, land breezes occurred in nearly all months. The mean number of monthly land breezes peaked in April and May at about 7, with a secondary maximum of 6–7 in July and August. The minimum of only 2 events per month occurred in December. Again, not all events may have been identified but these numbers are likely representative of the variations in land-breeze occurrence throughout the year.

Table 4.1. A summary of the number of land breezes identified by the objective algorithm for each month from February 1995 to January 2002. The months and year with a minimum number of land breezes are given by boldface type and are underlined, whereas the months and year with the maximum number of events are shown in bold italic font.

Year	Jan	Feb	Mar	Apr	May	Jun	Jul	Aug	Sep	Oct	Nov	Dec	Annual
1995		1	2	8	8	4	8	4	9	3	6	2	55
1996	4	6	2	9	4	8	5	5	6	5	2	4	60
1997	3	3	5	3	6	3	6	5	6	3	1	**0**	**44**
1998	1	3	2	5	12	6	7	3	**0**	3	5	2	49
1999	5	8	12	***13***	6	2	***13***	7	2	3	3	2	***76***
2000	2	2	8	6	6	2	5	9	2	6	5	3	56
2001	2	6	4	6	5	3	4	10	1	**0**	6	2	49
2002	4												(4)
Total	21	29	35	50	47	28	48	43	26	23	28	15	393
Average	3.0	4.1	5.0	7.1	6.7	4.0	6.9	6.1	3.7	3.3	4.0	2.1	56.1

The likely reasons why the land-breeze occurrence peaked in April are the prevalence of a surface high pressure ridge, the decreasing influence of synoptic-scale frontal systems and subsequent light surface winds, the increasing occurrence of daytime sea breezes, and the relatively large diurnal temperature variation. The maximum number of land breezes during July and August can be attributed to the nearly daily occurrence of sea breezes, which can retreat as a distinct convergence line during the evening and overnight hours. The smaller number of land breezes during December and January results from the greater frequency of synoptic-

scale fronts, stronger winds, and extensive cloud cover, which prevent the development of a land breeze.

The monthly distribution of all 393 land breezes along with the strongest events is shown in Fig. 4.1a. The total number of land breezes increased steadily from December to the peak month of April and remained near the maximum through August, with the exception of June. The frequency of land breezes decreased rapidly from August to September, and then again from November to December.

The strength of land breezes often varied substantially between events. Based on the subjective analysis prior to program development, "strong" land breezes were those events that had a distinct boundary passage and large directional wind shift across most of the tower network. "Weak" land-breeze events were often slow-moving, with a more subtle or gradual wind shift, and frequently affected only a portion of the tower network. Thus, the percentage of the towers that experienced a land-breeze passage in the network was used as a proxy for the strength of an event. In addition, land breezes were divided into five separate percentage categories of variable range (0 to 18%, > 18 to 33%, > 33 to 56%, > 56 to 79%, and > 79 to 100%) to ensure the same sample size in each bin.

In Fig. 4.1a, the frequency of the strongest land-breeze events (> 56% of the tower network experiencing a land-breeze passage) is plotted as a function of month (white bars). The frequency of strongest land-breeze events peaks in April with the broad maximum extending from February to May and a secondary maximum in July and August. Note the small number of strong land breezes from October to December.

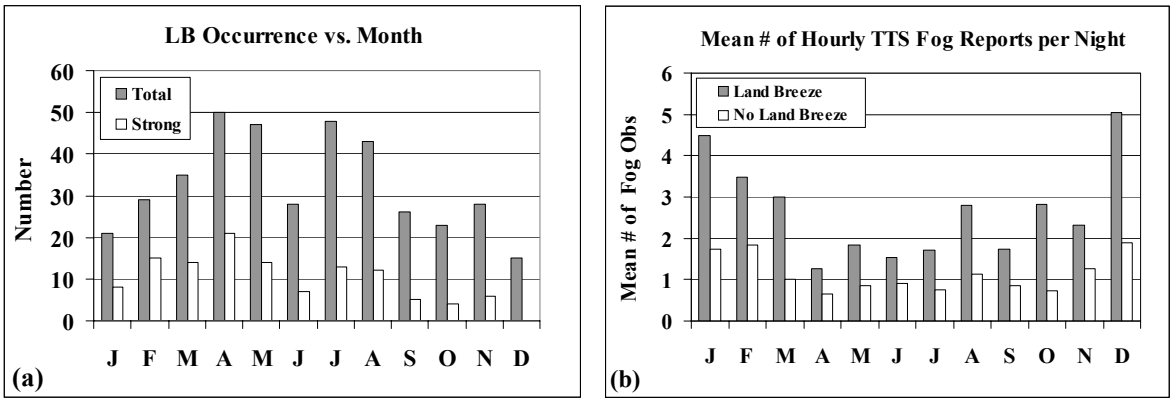

Figure 4.1. The monthly distributions of (a) land-breeze occurrences, and (b) mean number of nighttime hourly fog reports at TTS, valid from February 1995 to January 2002*. The strong land breezes in (a) includes the events that the objective program classified as having a land-breeze passage in at least 56% of the entire tower network.

The synoptic weather conditions conducive to land-breeze development in east-central Florida are also favorable for fog development (Wheeler et al. 1993). The land breeze coincided with a much higher occurrence of fog over east-central Florida, as seen in Fig. 4.1b. In every month, the mean number of fog observations at TTS associated with land breezes was approximately twice that of non-land breeze days. This amount of disparity could be a conservative estimate because out the 12 land-breeze events that the algorithm did not capture from the 1999–2000 season, the mean number of hourly TTS fog reports was 4.9 (not shown), considerably higher than most of the monthly means for land-breeze days shown in Fig. 4.1b.

4.1.2 Land-Breeze Directions

The direction from which the land breeze moved was determined objectively by averaging the wind direction for one hour after the land-breeze frontal passage at all towers that experienced the passage. Similarly, the pre-land breeze mean wind was determined for the hour prior to land-breeze passage at all towers that experienced the passage. These results were supplemented with subjective analyses for events that were quite weak, nearly stationary, or occurred prior to 0100 UTC or after 1200 UTC such that the objective

*The years of 1995 to 2001 were used for the climatology with the exception of January, which included data from the years 1996 to 2002 due to a format change in the archived KSC/CCAFS tower data in late January 1995.

algorithm could not compute the mean wind direction for an hour of time, since the defined analysis time window was 0000 to 1300 UTC.

During the fall months, land breezes were most common from the NW whereas land breezes from the SW and W were most prevalent in the spring and summer (Fig. 4.2a). Land breezes during the winter months are uniformly distributed among SW, W, and NW, slightly favoring the NW direction. The NW land breezes experience a maximum in October and November and a secondary maximum in March. Meanwhile, the frequency of SW and W land breezes increases gradually from December to March and then dramatically from March to April (Fig. 4.2a). Land breezes from the S were uncommon during all months.

The pre-land-breeze wind directions do not show such clear tendencies; however, some discernable relationships do exist. The distribution of pre-land-breeze winds from the N as a function of month closely follows the frequencies of the NW land-breeze directions (Fig. 4.2b). N winds were most common prior to the land breeze during October and November while S winds occurred most frequently prior to a land breeze from April to August. South and southeasterly winds were by far the most common prior to a land breeze from April to July. In general, E and NE winds were relatively uncommon prior to a land-breeze frontal passage.

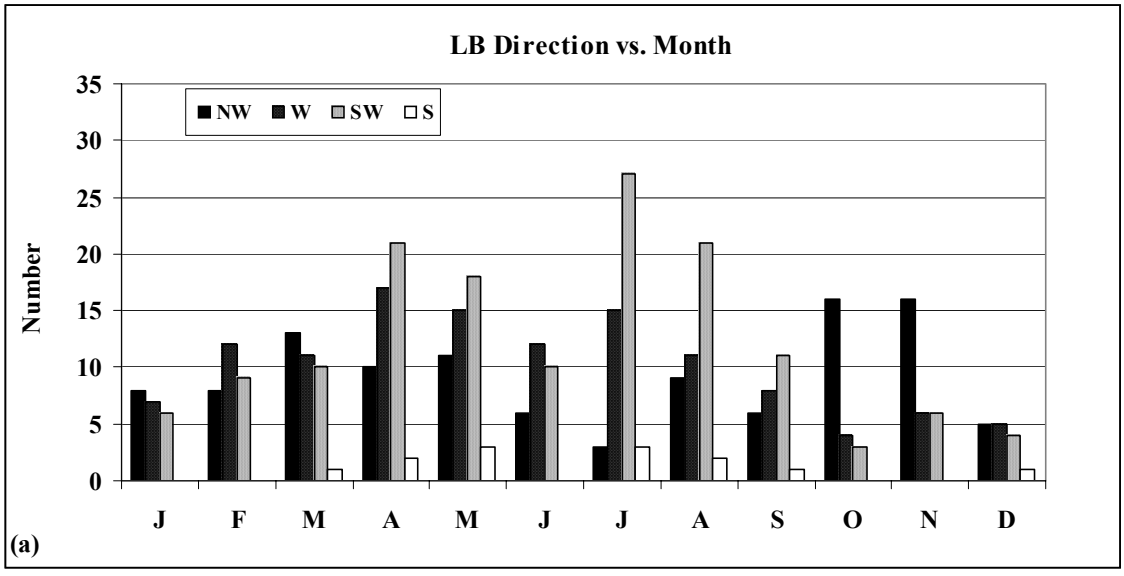

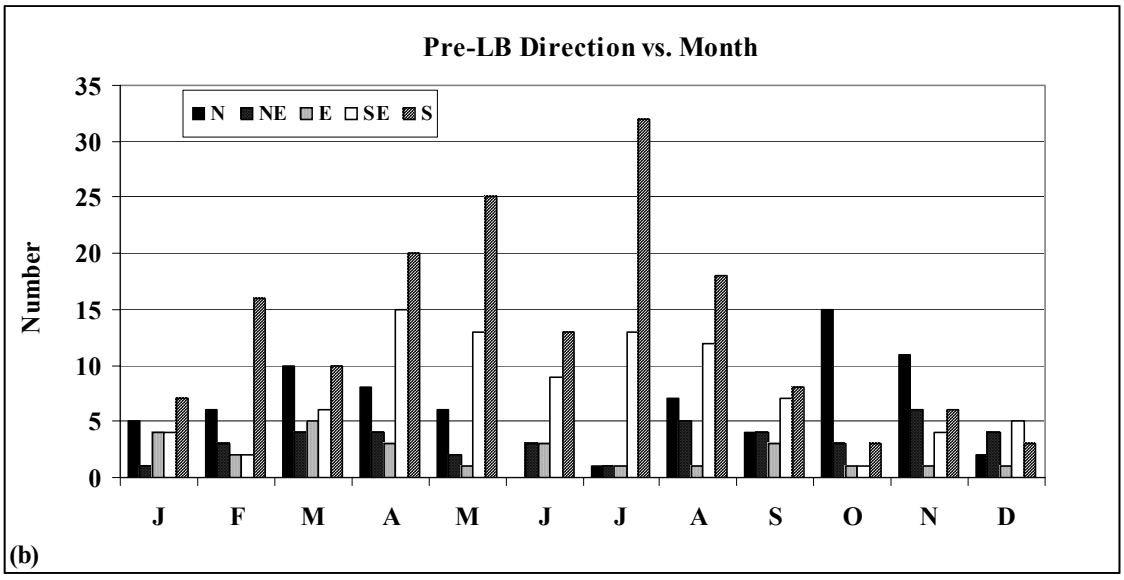

Figure 4.2. The distributions of the post-land breeze and pre-land-breeze wind direction as a function of month. (a) The monthly distributions of post-land-breeze directions for all events, and (b) the monthly distributions of pre-land-breeze directions for all events from February 1995 to January 2002. The land-breeze direction is given by the mean wind for one hour following the land-breeze frontal passage at all towers that experienced a land-breeze frontal passage.

4.1.3 Onset Times

Figure 4.3 shows the mean land-breeze onset time in hours after sunset for each month as well as the variation of the mean onset time versus pre- and post-land-breeze directions. During September to January, the mean onset time was between 6.0 and 8.0 hours after sunset whereas the average onset time was between 4.0 and 5.3 hours after sunset from February to August (Fig. 4.3a). According to Fig. 4.3b, land breezes coming from the NW had the latest mean onset times year-round, whereas the SW land breezes had the earliest mean onset time, particularly during the peak convective months (PC, June to September). The S and SE winds preceding a land breeze tended to have the earliest onset time (particularly during the PC months); however, the E, NE, and N winds preceding a land breeze had fairly uniform mean onset times for both minimal convective (MC, October to May) and PC months (Fig. 4.3b).

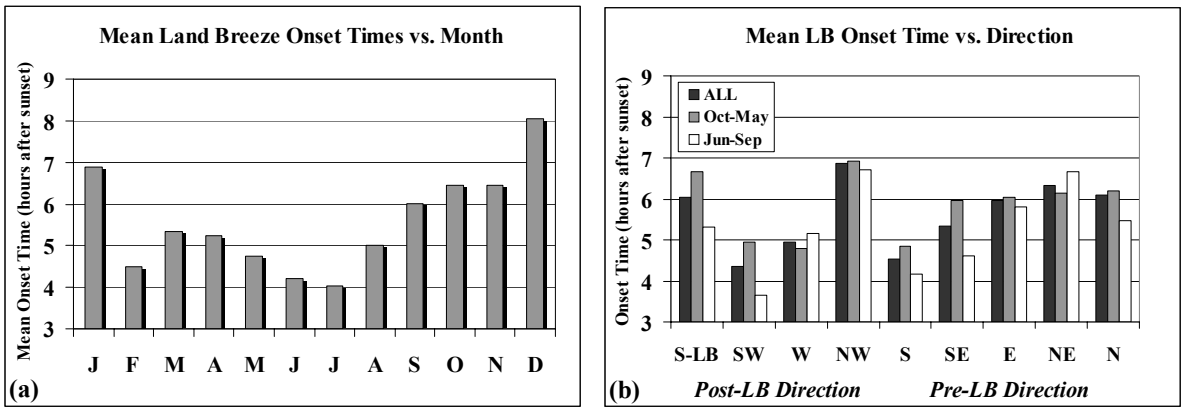

Figure 4.3. The mean land-breeze onset time as a function of (a) month, and (b) post-land breeze and pre-land breeze wind directions. The onset times are given in hours after sunset and the mean onset times in (b) are shown for all events, minimal convective months (October to May) and peak convective months (June to September).

The distribution of land-breeze onset times has a large spread, ranging from near sunset to 14 hours after sunset (e.g., at or slightly after sunrise in some instances; Fig. 4.4a). The primary maximum in land-breeze onset time is between 3 and 6 hours after sunset for both the MC (gray bars) and PC months (white bars), with secondary peaks at 8 and 11 hours after sunset. A general decreasing trend in the frequency occurred after 6 hours.

In Fig. 4.4b, the land-breeze onset times were distributed according to the occurrence (SB) or absence of a sea breeze (No SB) during the afternoon preceding the land breeze. From 0 to 5 hours after sunset, the land breezes following sea breezes occurred much more frequently, particularly in the 0–2 hour time frame. Beyond 6 hours, the land breezes without any preceding sea breezes were more common, with the exception of 8 and 11 hours after sunset (Fig. 4.4b). It appears that hours 8 and 11 were anomalies from the general trend after 6 hours; at all other times between 7 and 14 hours, the No SB land breezes occurred much more frequently than the SB land breezes.

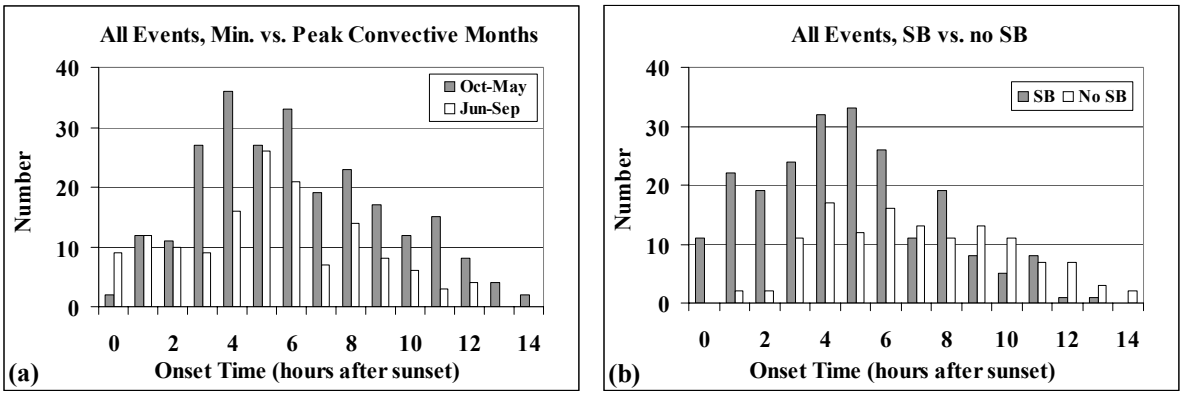

Figure 4.4. The frequency distribution of land-breeze onset times in hours after sunset for (a) minimal convective (October to May) versus peak convective months (June to September), and (b) land-breeze events with a sea breeze during the previous afternoon (SB) versus events without a sea breeze during the previous afternoon (No SB).

4.2 Analysis at Tall Tower 313

This section summarizes the characteristics of 264 land breezes that impacted Tower 313 from 1995 to 2001, and examines the differences between deep and shallow land-breeze circulations. The vertical depth of land-breeze circulations can vary a substantial amount from one event to the next, as seen in the case studies shown in Section 3. In order to understand the different characteristics associated with the various circulation depths, all land-breeze events that impacted Tower 313 were examined and classified into deep versus shallow events. Deep events were considered those in which the offshore wind component occurred at all observation levels of Tower 313 through 492 ft. The deep events typically had steeply-sloped transitions between onshore and offshore winds in the time-height cross sections, as well as stronger offshore wind speeds. The shallow events had an offshore flow depth less than 492 ft and often had a gradual slope at the leading edge of the front.

4.2.1 Onset Times at Tower 313

Tables 4.2 and 4.3 provide summary statistics of the overall distributions of onset times associated with deep versus shallow events, and SB versus No SB events, respectively. The greatest amount of disparity was found among deep versus shallow land breezes, regardless of the time of year. The mean onset time for deep events is over 4 hours earlier than that for shallow events for all months (Table 4.2). The deep events are slightly skewed towards earlier times, with a maximum time of 10.12 hours after sunset compared to 13.80 hours after sunset for the shallow events. It is important to note that 81% of the deep events had a sea breeze during the preceding afternoon whereas only 36% of the shallow events had a preceding sea breeze (Table 4.2). This sharp disparity in sea-breeze occurrence prior to the land breeze was prevalent in both the MC and PC months.

Based on this disparity in sea-breeze occurrence between deep and shallow events, the onset-time statistics for SB versus No SB days were also analyzed, with the results shown in Table 4.3. The statistics have similar characteristics as with the deep versus shallow comparison; however, the timing differences are not as substantial. The mean land-breeze onset time for SB events is only slightly more than 2.5 hours earlier than No SB events (Table 4.3). The minimum, maximum, and quartiles also indicate less disparity among the skewness of the different distributions. These results suggest that other mechanisms besides the sea-breeze occurrence/absence must have contributed to the development of deep versus shallow land breezes.

Table 4.2. A summary of the statistical properties of the onset time for deep and shallow land breezes at Tower 313, based on events with a preceding sea-breeze occurrence (SB) or absence (No SB) during all months, minimal convective months (Oct–May), and peak convective months (Jun–Sep). Deep land-breeze circulations had offshore winds at all levels of Tower 313 (up to at least 492 ft) and shallow circulations had offshore winds through a depth less than 492 ft. Onset times are given in hours after sunset.

Parameter	*Deep: All*	*Shallow: All*	*Deep: Oct-May*	*Shallow: Oct-May*	*Deep: Jun-Sep*	*Shallow: Jun-Sep*
Number of Days	150	114	84	78	66	36
Mean Time	4.42	8.59	4.55	8.70	4.26	8.34
Minimum Time	-0.27	3.23	0.88	3.32	-0.27	3.23
1st Quartile	3.03	6.98	3.15	6.95	2.35	7.33
Median	4.35	8.93	4.35	8.98	4.26	8.43
3rd Quartile	5.90	10.33	5.98	10.74	5.79	9.72
Maximum Time	10.12	13.80	8.57	13.80	10.12	11.80
SB	122	41	66	24	56	17
No SB	28	73	18	54	10	19
% SB	81.3%	36.0%	78.6%	30.8%	84.8%	47.2%

Table 4.3. A summary of the statistical properties of the onset time associated with land breezes that had a preceding sea-breeze occurrence (SB) versus absence (No SB) at Tower 313. Onset times are given in hours after sunset.

Parameter / Statistic	*SB*	*No SB*
Number of Days	163	101
Mean Time	5.24	7.80
Minimum Time	-0.27	1.67
1st Quartile	3.19	5.81
Median	4.97	7.83
3rd Quartile	6.89	9.83
Maximum Time	13.52	13.80

The distributions of onset times for deep versus shallow and SB versus No SB events are shown explicitly in Fig. 4.5. The timing differences between deep and shallow land breezes are evident in Fig. 4.5a. The deep land-breeze events peak sharply between 3 and 7 hours after sunset with very few occurrences after 9 hours. Meanwhile, the shallow land breezes have a more broad maximum between 7 and 12 hours after sunset along with no occurrences before 4 hours.

Deep land breezes were typically preceded by a sea breeze during the previous afternoon (Fig. 4.5b). Deep circulations were much more uncommon when not associated with a preceding sea breeze. The SB deep circulations appear to be normally distributed about a mean of ~ 4–5 hours. Meanwhile, the No SB deep circulations do not appear to be normally distributed, and tended to occur after 3 hours; however, the sample size of the No SB deep events was quite small. Converse to the deep circulations, the shallow land breezes were more often not associated with preceding sea breezes as few differences occur in the distributions of onset time between SB and No SB events (Fig. 4.5c).

Finally, Fig. 4.5d shows the timing of SB events in hours between the SB and land-breeze onset times for both deep and shallow circulations. Clearly, the deep land breezes tended to begin earlier than the shallow land breezes, with most deep events occurring between 10 and 14 hours after the SB onset time. The majority of shallow land breezes following a SB occurred between 16 and 20 hours after the SB onset time. This large time separation was typically caused by an early SB onset time followed by a late land-breeze onset time during onshore (easterly) synoptic flow. Again, the deep land breezes were much more common when following a SB.

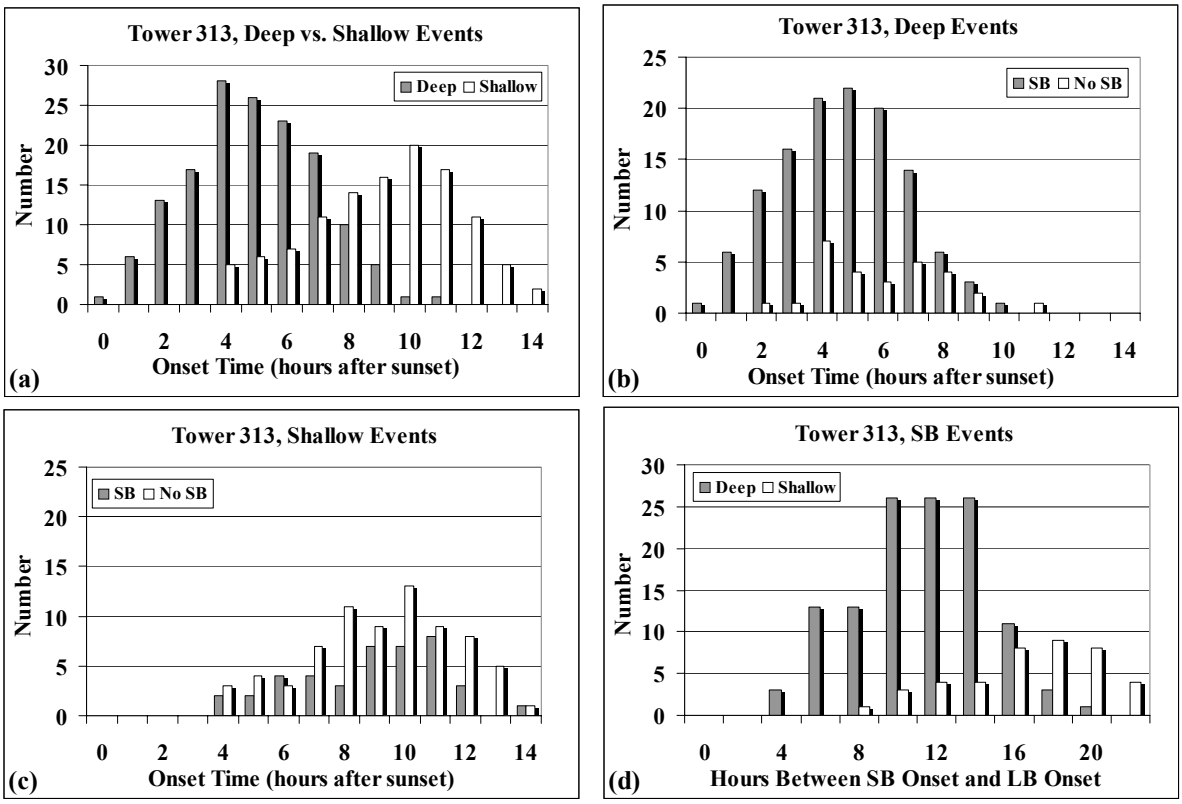

Figure 4.5. The distributions of land-breeze onset times (in hours after sunset) at Tower 313 for all months from February 1995 to January 2002. The distributions are shown for (a) deep (> 492 ft depth) versus shallow (< 150 m depth) circulations, (b) the occurrence (SB) / absence (No SB) of a sea breeze during the afternoon preceding the land breeze for all deep circulations, and (c) SB / No SB during the afternoon preceding the land breeze for shallow circulations. In (d), the distribution of elapsed times between the SB and LB onset times are shown for deep versus shallow events for all land breezes that had a sea breeze during the preceding afternoon.

4.2.2 Land-Breeze Directions at Tower 313

The pre- and post-land breeze wind directions also show some disparity between deep and shallow, and SB versus No SB events. According to Fig. 4.6a, nearly all land breezes at Tower 313 that came from the NW were shallow events, especially during the MC months. Meanwhile, about twice as many deep land breezes came from the SW compared to shallow land breezes in both the MC and PC months. For the pre-land breeze wind direction, the greatest disparity is found in the N and S categories. When N winds preceded a land breeze during the MC months, most events tended to be shallow, but when S winds preceded a land breeze at any time of the year, most land breezes had a deep circulation (Fig. 4.6b). This distribution indicates that the most common wind regimes associated with land breezes were S winds shifting to SW or W, and N winds shifting to NW after the land-breeze passage, consistent with the subjective analysis.

Next, the wind directions associated with deep and shallow circulations were examined separately for SB versus No SB events. The SW and W land-breeze directions for SB days were the most common categories for deep circulations (Fig. 4.6c). The next most frequent types of deep land breezes were W and SW directions for No SB days. The NW land breezes rarely had deep circulations. The most prevalent pre-land breeze wind

directions for deep circulations were S and SE winds for SB days (Fig. 4.6d). The S and SE pre-land breeze directions for SB days comprised 87% of the deep/SB events, and 71% of all deep events (SB and No SB).

For shallow land-breeze circulations, the pre- and post-land-breeze wind directions are more evenly distributed compared to deep land breezes, but still favor particular categories. The most prevalent shallow land breezes came from the NW during the MC months and were not associated with a SB, followed by W and SW directions also not associated with a SB (No SB: Oct–May in Fig. 4.6e). For shallow land breezes during SB days, the occurrence is evenly distributed among the NW, W, and SW directions. Finally, the pre-land breeze wind direction for shallow events are well distributed across all categories. The most common directions preceding the land-breeze front were N and S for No SB cases during the MC months (Fig. 4.6f). Otherwise, no category of pre-land breeze wind direction was favored for shallow events at Tower 313.

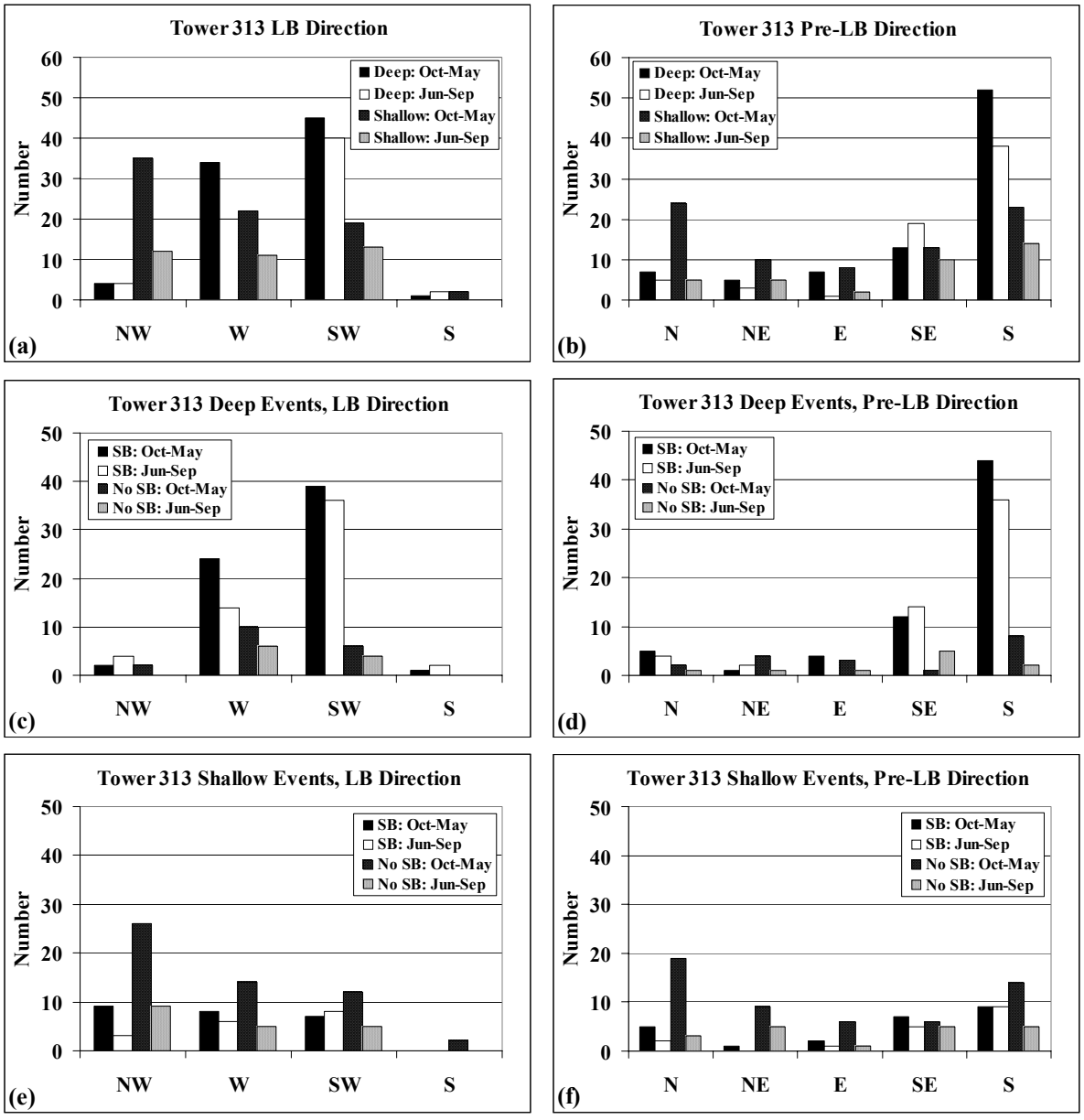

Figure 4.6. The distribution of post-land breeze (LB) and pre-LB wind directions at Tower 313 during the MC months (October to May) and PC months (June to September) for the following combinations: (a) LB direction for deep versus shallow events, (b) Pre-LB direction for deep versus shallow events, (c) LB direction of deep events for the occurrence (SB) versus absence of a sea breeze (No SB) during the preceding afternoon,

(d) Pre-LB direction of deep events for SB versus No SB, (e) LB direction of shallow events for SB versus No SB, and (f) Pre-LB direction of shallow events for SB versus No SB. Note that the y-axis ranges from 0 to 60 in (a) and (b), and from 0 to 50 in (c) through (f).

4.3 Composite Changes in Temperature, Stability, Winds, and Relative Humidity

To determine the mean impact of land breezes on the temperature, moisture, and wind fields, composite changes were generated by averaging the variations in each quantity at tower locations that experienced a land-breeze passage. The values were averaged every 5 minutes at ± 60 minutes of the land-breeze frontal passage. The composite quantities normalized to the time of the land-breeze passage isolate the impact of the land breeze.

4.3.1 Minimal Convective Months (October to May)

Figures 4.7a-b show the mean 6-ft and 54-ft temperature cooling rates within ± 60 minutes of land-breeze passages during the MC months. Each event was categorized into NW, W, and SW land breezes based on the mean wind direction for the hour after passage at all towers that experienced the land breeze. The mean cooling rate was then calculated for the NW, W, SW, and all land-breeze events (ALL).

At 6 ft, land breezes during the MC months tended to have a warming effect, particularly for events with W winds behind the boundary (Fig. 4.7a). For the hour prior to the land breeze (-60 to 0 minutes), the mean temperature change rate at 6 ft was about -1°F h^{-1}. After the boundary passage, the W land breezes experienced a warming rate of about 0.5°F h^{-1} for approximately 30 minutes. The NW land breezes had a smaller impact on 6-ft temperatures since their passage only slowed the rate of cooling for the first 30 minutes, with a slight warming rate thereafter. The SW land breeze had the smallest impact on the mean temperature change rate of the 6-ft temperatures.

At 54 ft, all land-breeze passages during the MC months had a net cooling effect on the temperatures, with the W land breeze having the largest impact in the hour after passage (Fig. 4.7b). In fact, the mean 54-ft temperature change for each land breeze regime was nearly opposite to the 6-ft temperature change. The W (SW) land breeze had the greatest (least) warming influence at 6 ft, whereas the W (SW) land breeze had the greatest (least) cooling impact at 54 ft. At both heights, the NW land breeze aligned most closely with the overall mean temperature change rates (ALL in Fig. 4.7b).

The difference between the 54-ft and 6-ft temperatures, representing stability in this layer, also showed variations between the different land breezes. The near-surface layer was almost always stable prior to land-breeze passages ($T_{54} > T_6$), due to light winds generating conditions favorable for development of a radiation inversion. The land-breeze passages, however, acted to decrease the 6 to 54-ft stability due to the mechanical mixing associated with the leading edge of the land-breeze front. As seen in Fig. 4.7c, the near-surface layer was the least stable during nights with SW land breezes, and the SW land-breeze passage also had the least impact on the rate of stability decrease (Fig. 4.7d). The W and NW land breezes had comparable low-level stability values (Fig. 4.7c); however, the W land breeze experienced the largest and most sustained rate of decrease in the stability (Fig. 4.7d). These results suggest that a W land breeze would have the strongest impact on stability decrease and that a SW land breeze would have the least influence on temperatures and near-surface stability across KSC/CCAFS.

The composite wind direction and speed graphs also show a distinct signal about the land-breeze frontal passage, as given in Fig. 4.8. By definition, the objective land-breeze identification algorithm searched for sharp wind-shift lines; therefore, one would expect to see a large absolute change in the wind direction centered on the land-breeze passage. Figure 4.8a shows the significant maximum in the absolute value of the wind direction change, centered on the land-breeze passage. The average wind direction changes gradually decrease from about 10 to 60 minutes after the land-breeze passage back down to about 10–15°. The W land breezes have the largest absolute wind direction change at the land-breeze onset time, and the SW land breeze has the least absolute wind direction change (Fig. 4.8a).

In the composite wind-speed graph of Fig. 4.8b, the speed reaches a minimum at the time of the land-breeze frontal passage, due to convergence along the leading edge of the front. The SW land breezes tended to have a decrease in wind speed of about 1 to 2 kt following the land breeze passage; however, this direction had the strongest winds speeds overall, likely due to the predominance of deep circulations and post-sea breeze

flow prior to the SW land-breeze onset. The NW and particularly the W land breezes had an increase in the wind speeds following the land-breeze frontal passage. The NW land breeze had the lowest overall wind speeds, consistent with the earlier results in this section indicating that the NW land breeze tended to be the weakest among all land-breeze directions.

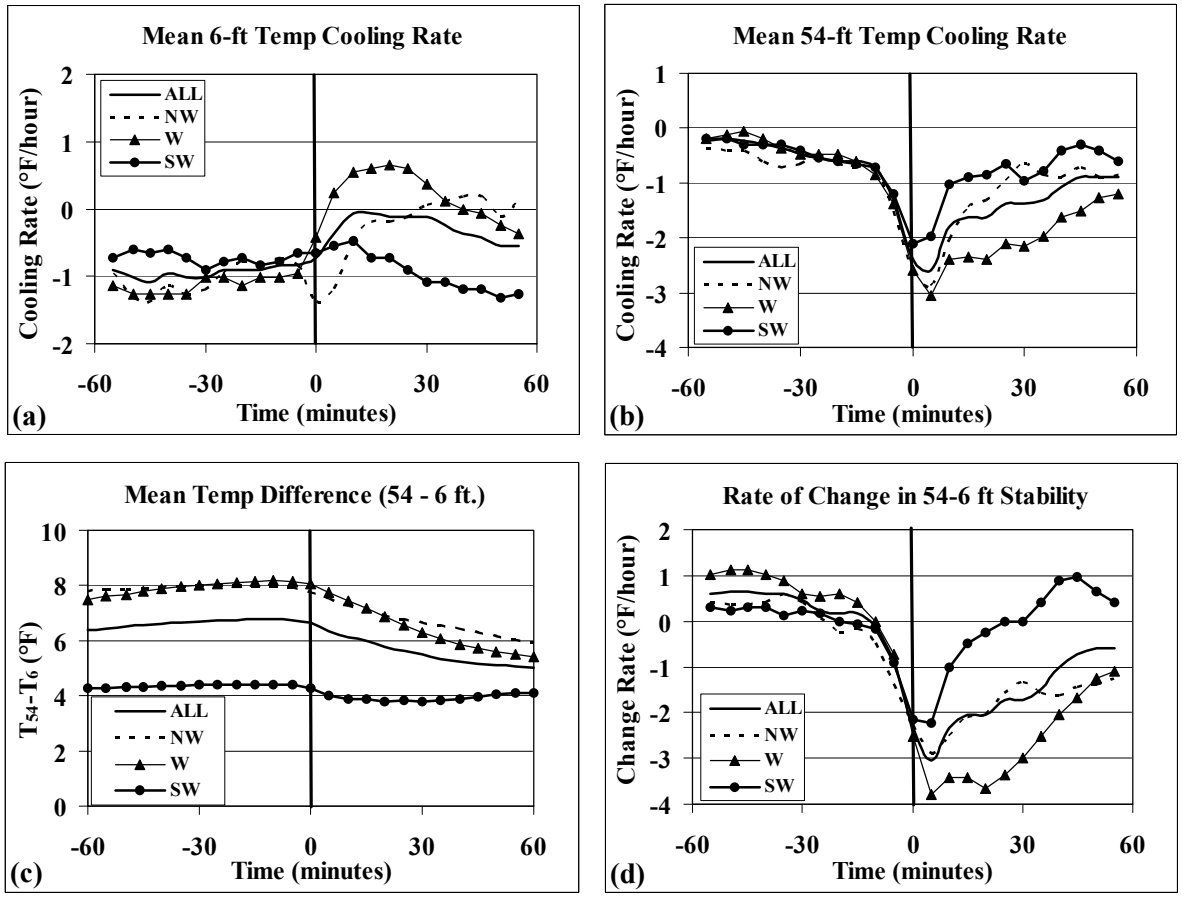

Figure 4.7. Five-minute mean temperature variations at ± 60 minutes relative to land-breeze passages during the MC months (October to May) for all land breezes (ALL), and for events with post-land breeze winds from the northwest (NW), west (W), and southwest (SW). (a) 6-ft temperature change rate (°F h^{-1}), (b) 54-ft temperature change rate (°F h^{-1}), (c) the mean difference between the 54-ft and 6-ft temperatures (layer stability, $T_{54} - T_6$ in °F), and (d) the rate of change in the difference between the 54-ft and 6-ft temperatures (rate of change in stability, °F h^{-1}). Temperature-change and stability-change rates were computed every 5 minutes using centered differences. The bold vertical line at 0 minutes in each panel represents the time of the land-breeze passage.

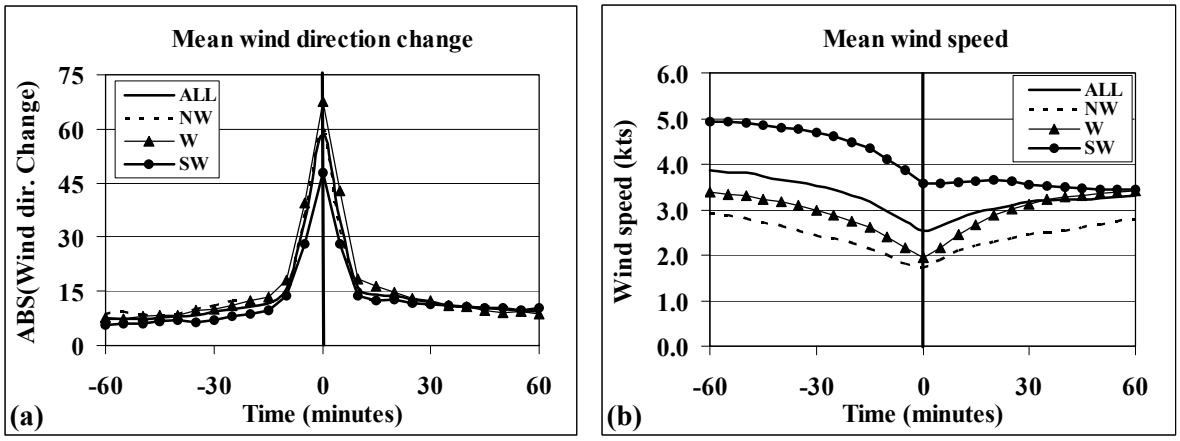

Figure 4.8. Five-minute mean wind variations at ± 60 minutes relative to land-breeze passages during the MC months (October to May) for all land breezes (ALL), and for events with post-land breeze winds from the northwest (NW), west (W), and southwest (SW). (a) the absolute value of 54-ft wind direction changes (degrees), and (b) the 54-ft wind speed (kt). The bold vertical line at 0 minutes in each panel represents the time of the land-breeze passage.

The composite 6-ft relative humidity chart at ± 60 minutes of land-breeze passages during the MC months is provided in Fig. 4.9. Among all sensible surface variables, the relative humidity experienced the least impact from land breezes. The mean relative humidity in the hour prior to the land breeze steadily increased about 2% in all instances (Fig. 4.9a). In the hour following the land-breeze passage, the relative humidity tended to level off in the W and NW land breezes, but continued to increase about 1.5% in the SW land breezes. Again, the SW land breeze had disparate characteristics compared to the W and NW land breezes, having about a 2% lower mean relative humidity overall.

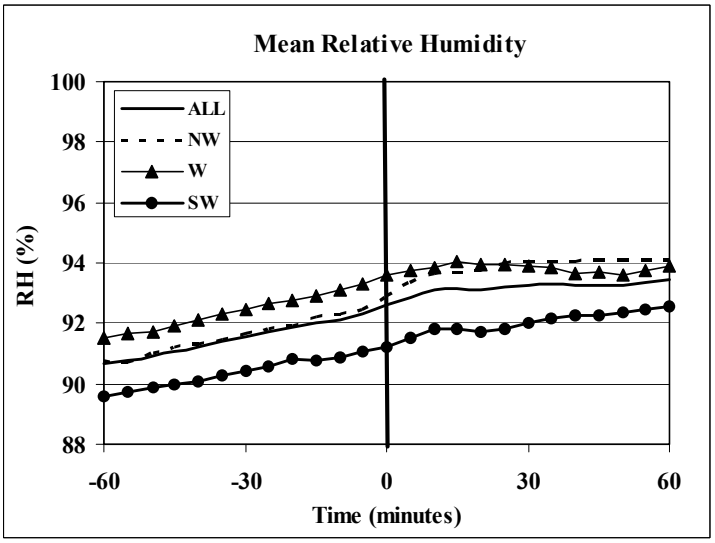

Figure 4.9. Five-minute mean 6-ft relative humidity variations at ± 60 minutes relative to land-breeze passages for all land breezes (ALL), and for events with post-land breeze winds from the northwest (NW), west (W), and southwest (SW), valid during October to May. The bold vertical line at 0 minutes in each panel represents the time of the land-breeze passage.

4.3.2 Peak Convective Months (June to September)

The ± 60 minutes composite charts for the PC months of June to September show similarities as well as some differences from the MC composite charts. As in the MC months, the 6-ft temperatures experienced about a -1° F h^{-1} temperature change rate prior to land-breeze passage; however, for the hour following the land-breeze onset, the temperature change rate increased only gradually (Fig. 4.10a), unlike the rather abrupt change in the rate shortly after the land-breeze passage during the MC months (Fig. 4.7a). The exception is in the SW land breezes, which did not experience much change in the temperature change rate for both MC and PC months.

The 54-ft temperature change rate during the PC months is much different than MC months, except for NW land breezes. The 54-ft temperature change rate for W and SW land breezes remained nearly constant following the land-breeze passage whereas the NW land breeze had a brief increase in cooling (Fig. 4.10b). A comparison between the 54-ft temperature change rates of the MC (Fig. 4.7b) and PC land breezes suggests that land breezes during the cooler, dryer MC months tended to be driven more by density-current dynamics (i.e. land–sea thermal contrasts), whereas the land breezes during the PC months were generally not driven by density-current dynamics (except for possibly the NW land breeze).

As expected, the low-level stability between 6 ft and 54 ft was, on average, lower during the PC months (Fig. 4.10c). Similar to the MC results in Fig. 4.7c, the stability was lowest for SW land breezes. Only the NW land breeze during the PC months resulted in any substantial decrease in the mean stability of this layer following the land-breeze passage. The stability change in the NW land breezes is more clearly seen in Fig. 4.10d, which shows a rather sharp decrease in the stability rate of change immediately before and at the time of onset, followed by a gradual increase in the rate. Compared to the MC months where the near-surface stability decreased abruptly at the time of land-breeze passage, the near-surface stability changes associated with land breezes during the PC months were much smaller.

The composite wind direction and speed changes during the PC months (Fig. 4.11) closely resemble the results of the MC months in Fig. 4.8. The mean wind-direction change has a distinct maximum at the time of the land breeze passage (by definition) and the wind-speed composite has a minimum due to convergence at the land-breeze front. These results are nearly identical to the MC months.

Finally, the mean relative humidity composite graphs during the PC months (Fig. 4.12) also closely resemble the results from the MC months (Fig. 4.9). The only difference worth noting is that the overall mean relative humidity was about 2% greater during the PC months compared to the MC months.

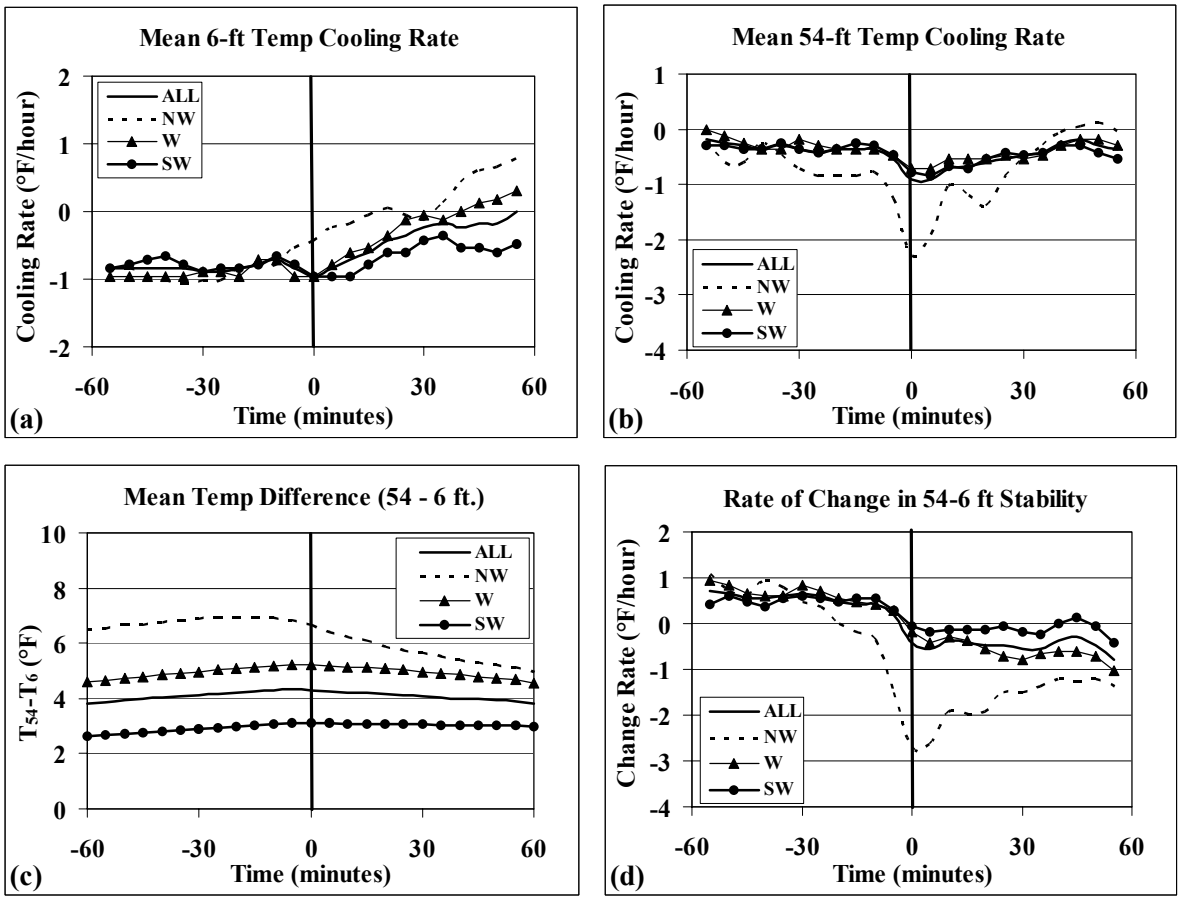

Figure 4.10. Five-minute mean temperature variations at ± 60 minutes relative to land-breeze passages during the PC months (June to September) for all land breezes (ALL), and for events with post-land breeze winds from the northwest (NW), west (W), and southwest (SW). (a) 6-ft temperature change rate (°F h^{-1}), (b) 54-ft temperature change rate (°F h^{-1}), (c) the mean difference between the 54-ft and 6-ft temperatures (layer stability, $T_{54} - T_6$ in °F), and (d) the rate of change in the difference between the 54-ft and 6-ft temperatures (rate of change in 54–6 ft stability, °F h^{-1}). Temperature-change and stability-change rates were computed every 5 minutes using centered differences. The bold vertical line at 0 minutes in each panel represents the time of the land-breeze passage.

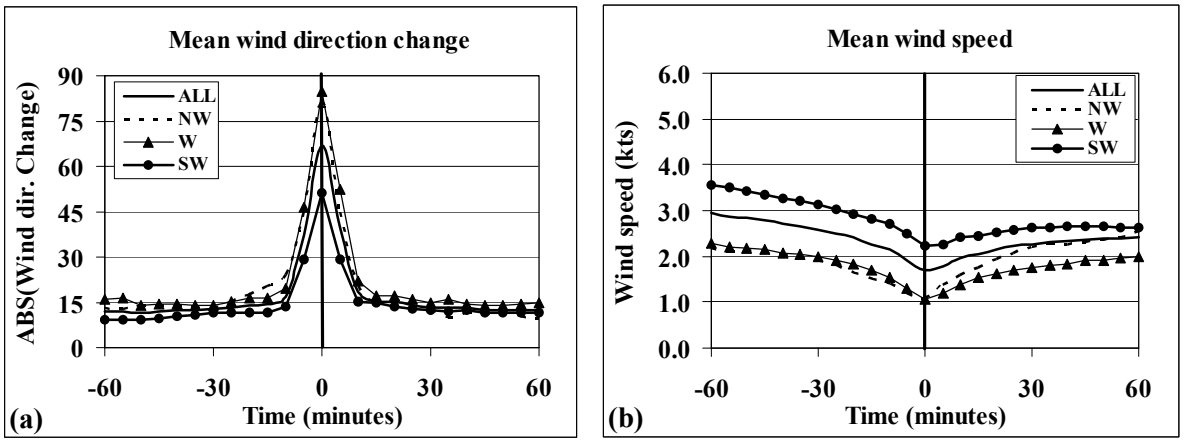

Figure 4.11. Five-minute mean wind variations at ± 60 minutes relative to land-breeze passages during the PC months (June to September) for all land breezes (ALL), and for events with post-land breeze winds from the northwest (NW), west (W), and southwest (SW). (a) the absolute value of 54-ft wind direction changes (degrees), and (b) the 54-ft wind speed (kt). The bold vertical line at 0 minutes in each panel represents the time of the land-breeze passage.

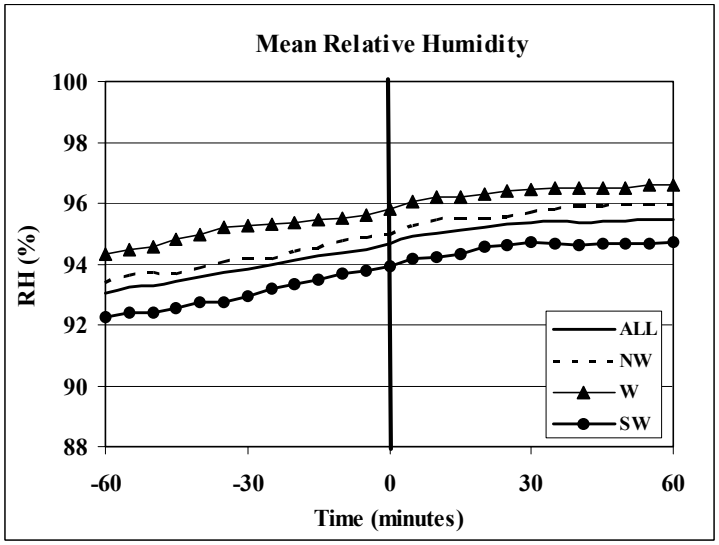

Figure 4.12. Five-minute mean 6-ft relative humidity variations at ± 60 minutes relative to land-breeze passages for all land breezes (ALL), and for events with post-land breeze winds from the northwest (NW), west (W), and southwest (SW), valid during June to September. The bold vertical line at 0 minutes in each panel represents the time of the land-breeze passage.

4.3.3 Summary of Composite Characteristics

The different composite characteristics between SW, W, and NW land breezes could be the result of the different land and terrain characteristics upstream of KSC/CCAFS. The terrain to the SW of KSC/CCAFS consists primarily of swamp lands with few forests or significant elevation, resulting in relatively little temperature contrast between the interior and the coastal regions. The most extensive forests in the Florida peninsula lie to the NW of KSC/CCAFS, as well as the highest elevation. It could be that the NW land breeze is a type of shallow, cool drainage flow originating from the higher elevations and forests near Ocala and Gainesville.

Meanwhile, the W and particularly the SW land breezes appeared to modulate the inertial oscillation, or the clockwise turning of the wind field caused by the Earth's rotation (Coriolis force). At the latitude of central Florida and in the absence of all other forces, it takes about 50 hours for the Coriolis force to rotate the wind field clockwise a full 360° (about 7.2° per hour). With a general absence of large-scale synoptic forcing, the winds tend to rotate clockwise to a S direction nearly parallel to the coast shortly after sunset, often associated with a sea-breeze circulation under a favorable land-sea temperature contrast. Depending on the balance between the mesoscale pressure gradient, advection, Coriolis force, and friction (Zhong and Takle 1993), the land breeze can develop, leading to a sudden, enhanced clockwise turning of the wind field beyond that caused by the Coriolis force alone.

5. Forecast Tools

This section describes the meteorological conditions favorable for a land-breeze front and provides a set of forecast tools that can be applied by forecasters. The forecast tools were developed from the results of the 7-year climatology, and includes an analysis of the 300 most distinct, clear-cut land breezes (180 events during the MC months and 120 events during the PC months) out of the 393 total events. For each of the 300 events analyzed, the MSLP field was examined at 0000 UTC on the day of the land breeze, and the prevailing synoptic flow direction was determined along with the magnitude of the pressure gradient across the length of the Florida peninsula. These large-scale flow characteristics, along with the sea-breeze occurrence/absence during the day preceding the land-breeze event, were used to categorize land-breeze events for various regimes in order to obtain a reliable set of forecast tools.

Section 5.1 first discusses the favorable meteorological conditions for a land-breeze occurrence and provides a flowchart that forecasters can use to determine the qualitative and quantitative likelihood of a land breeze. Sections 5.2 and 5.3 provide guidance for determining the land-breeze onset time and direction, respectively, given the synoptic surface flow and occurrence of a daytime sea breeze.

5.1 Land-Breeze Occurrence

Figures 5.1 and 5.2 are flowcharts that can help forecasters determine the likelihood of a land breeze on a given night. The conditions used to compile Figs. 5.1 and 5.2 are based on the subjective and objective results of the 7-year climatology from February 1995 to January 2002. The logic in the flowchart provides information about the synoptic and mesoscale conditions favorable for the development of a land breeze, as well as qualitative and quantitative information on the likelihood of a land-breeze occurrence, given existing and forecast meteorological conditions.

The conditions required for land-breeze development are depicted at the beginning of Figs. 5.1 and 5.2. There should be no precipitation across central Florida, mainly clear skies with no low cloud ceilings for most of the night, average 54-ft wind speeds less than 7 kt, and the absence of any significant large-scale pressure changes or troughs. A favorable synoptic setup is to have a ridge of high pressure in the vicinity of the Florida peninsula, or a high pressure center overhead. A favorable mesoscale criterion for land-breeze occurrence is to have a sea-breeze circulation during the previous afternoon. The majority of land-breeze frontal passages across KSC/CCAFS during the 7-year period (57%) followed a sea-breeze circulation from the preceding afternoon.

By following the logic in Figs. 5.1 and 5.2 and provided that all initial meteorological criteria are met, the most favorable scenarios for land-breeze occurrence are:

- Current month in the March to September range,
- Land-breeze occurrence in the previous night during May to September (e.g. persistence),
- Sea-breeze occurrence the previous afternoon during June to September, particularly in conjunction with offshore synoptic flow,
- Sea-breeze occurrence the previous afternoon during October to May in conjunction with offshore synoptic flow, or
- Onshore synoptic flow during October to May without a sea-breeze during the previous afternoon.

Conversely, the least likely scenarios for land-breeze occurrence are (provided that all initial meteorological criteria are met):

- Offshore synoptic flow without a sea breeze during the day for all months (i.e. synoptic flow is already offshore, thus precluding the development of a land-breeze wind shift),
- Light and variable synoptic flow without a sea breeze during the day for all months, or
- Current month is October, December, or January.

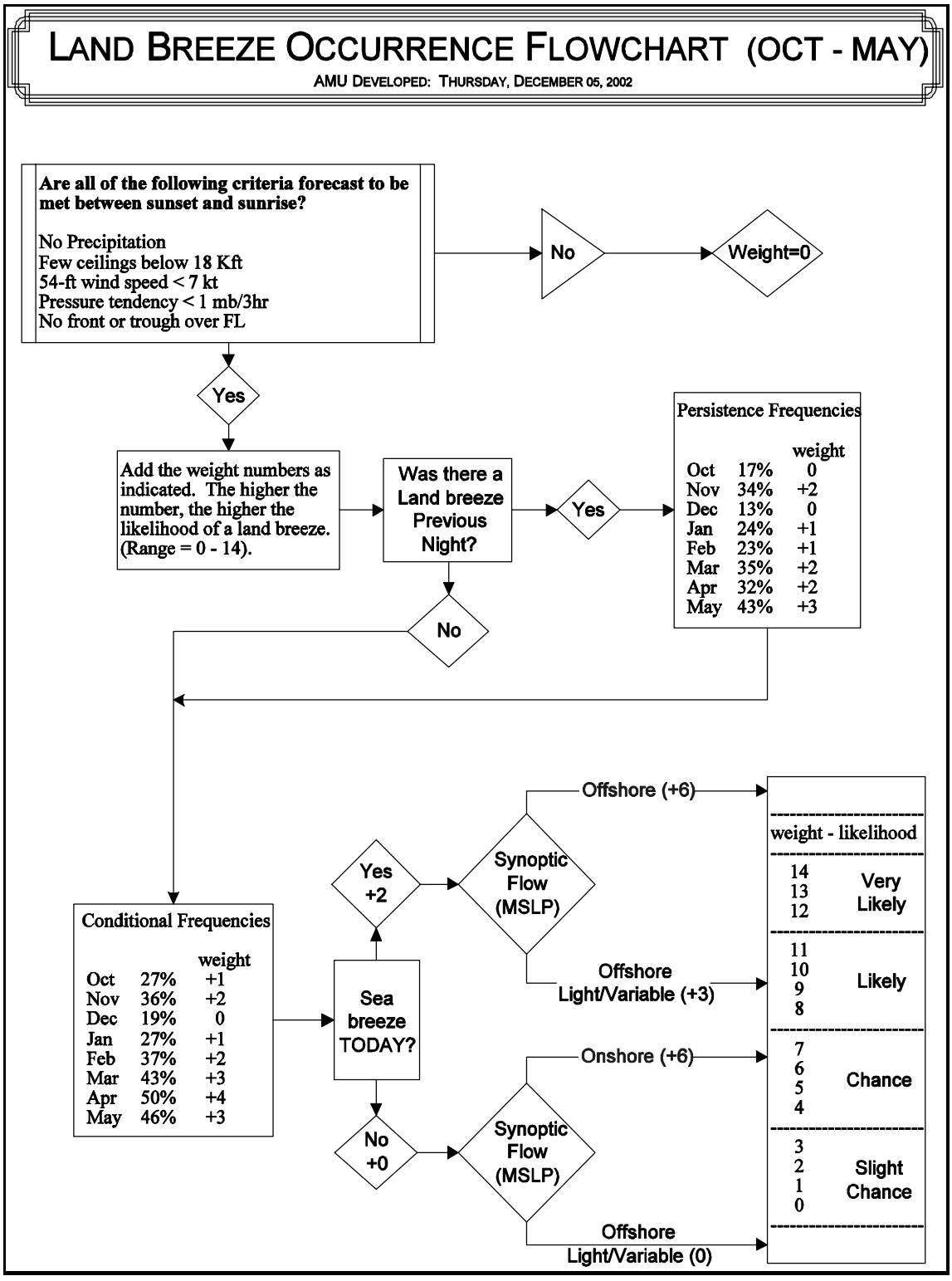

Figure 5.1. A flowchart for determining whether a night has the potential for a land breeze during the MC months. If all initial meteorological conditions are met, then the forecaster follows the logic of the chart and adds all weights together. The final number represents a qualitative measure of the likelihood of a land breeze, ranging from 0 (land breeze least likely) to 14 (land breeze most likely). The flowchart also provides the persistence and conditional frequencies for general land-breeze occurrence during each month, provided that all initial meteorological criteria are met.

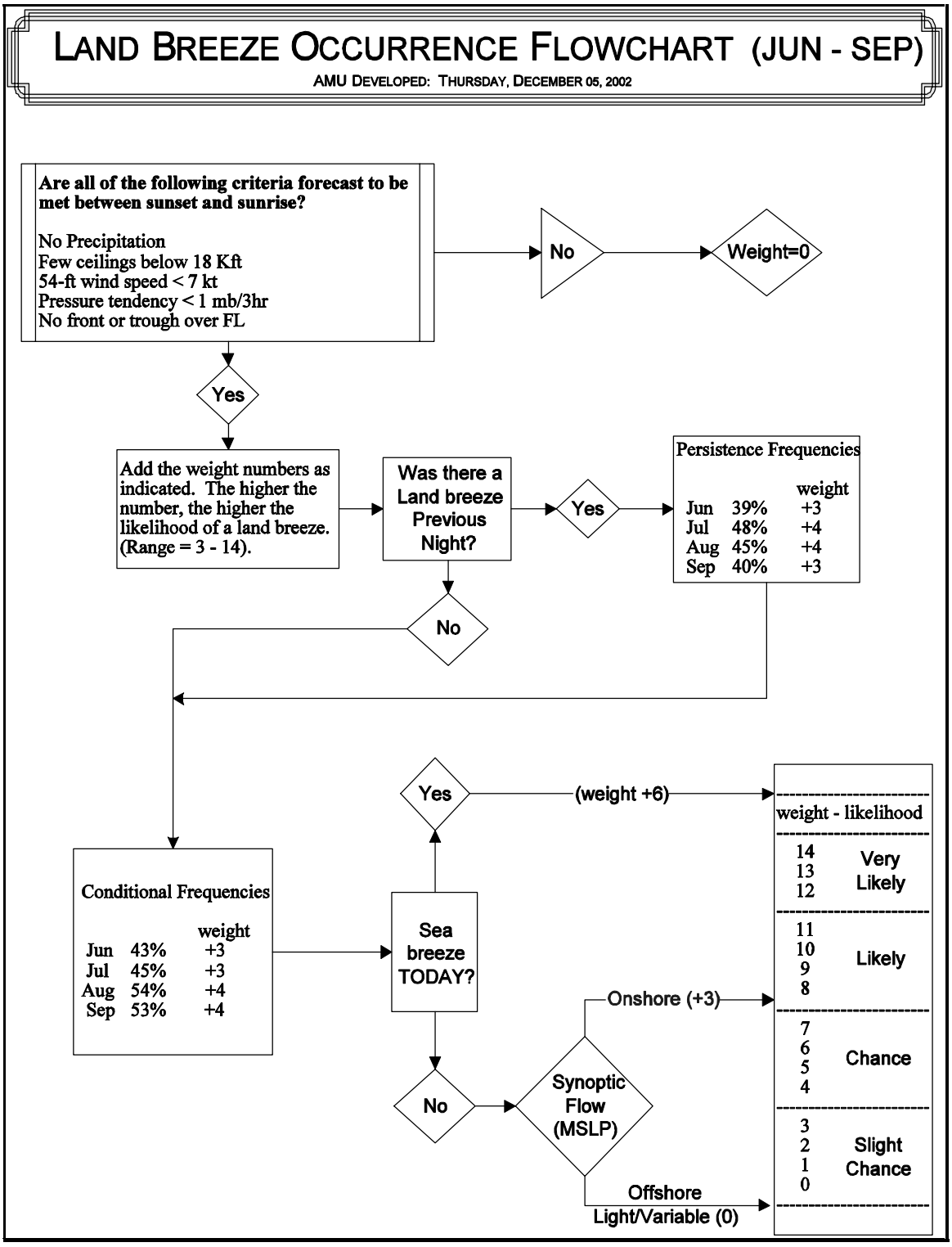

Figure 5.2. A flowchart for determining whether a night has the potential for a land breeze during the PC months. If all initial meteorological conditions are met, then the forecaster follows the logic of the chart and adds all weights together. The final number represents a qualitative measure of the likelihood of a land breeze, ranging from 0 (land breeze least likely) to 14 (land breeze most likely). The flowchart also provides the persistence and conditional frequencies for general land-breeze occurrence during each month, provided that all initial meteorological criteria are met.

5.2 Land-Breeze Onset Time

Figure 5.3 shows a series of scatter diagrams of the synoptic flow directions plotted against the land-breeze onset times in hours after sunset. On the y-axis, the numerical values represent the category of the synoptic flow, where 360° is N flow, 315° is NW flow, etc. It is important to note that the 0° direction represents light and variable flow, as the direction was not discernable on the MSLP chart. The separate panels in Fig. 5.3 are for all land-breeze events during the Minimal Convective (MC) months (Oct–May in Fig. 5.3a) and Peak Convective (PC) months (Jun–Sep in Fig. 5.3b); events preceded by a sea breeze for the MC months (Fig. 5.3c) and PC months (Fig. 5.3d); and events not preceded by a sea breeze for the MC months (Fig. 5.3e) and PC months (Fig. 5.3f).

In all plots of Fig. 5.3, it is evident that offshore flow led to earlier onset times of the land breeze and onshore flow led to later onset times. For flow from the SW, W, and NW (225° to 315°), the land breeze nearly always began between the local sunset time (0 hours) and 6 hours after sunset. This statement was true for all months out of the year. In addition, most of the early onset times were preceded by a sea-breeze circulation during the previous afternoon (SB Events in Figs. 5.3c-d) whereas very few land-breeze events occurred during offshore flow and No SB, particularly in the PC months (No SB Events in Figs. 5.3e-f).

The onshore flow typically yielded later onset times and larger spreads in the scatter distribution, particularly during the MC months (NE to SE, or 45° to 135° categories in Figs. 5.3a-b). The S flow direction (180°) appears to be a transition zone between the earlier onset times with offshore flow and later onset times with onshore flow. Land-breeze frontal passages occurred with or without a preceding sea breeze in onshore flow during any part of the year, but were particularly common during the MC months for No SB events (Fig. 5.3e). The occurrence or absence of a preceding sea breeze during onshore flow does not help to discriminate the onset time, as the distributions are quite spread out, particularly during the MC months (Figs. 5.3c-f). However, no land-breeze events during onshore flow began prior to 4 hours after sunset during the PC months, and very few events occurred before 3 hours after sunset during the MC months.

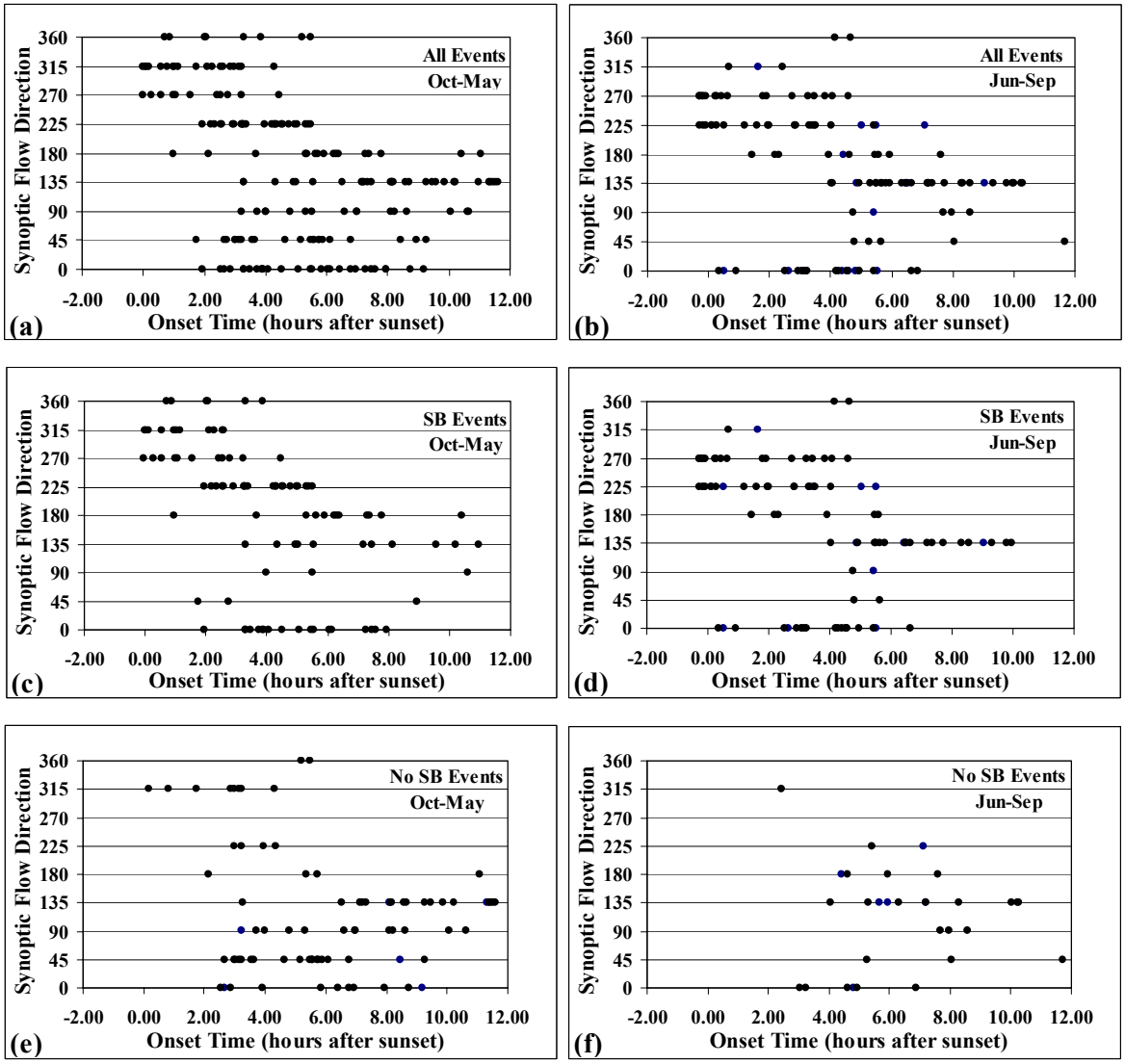

Figure 5.3. The distributions of the surface synoptic flow versus the onset time of land breezes during February 1995 to January 2002. The distributions are shown for all events during the months of (a) October to May, and (b) June to September; events preceded by a sea breeze (SB) during the months of (c) October to May, and (d) June to September; and events not preceded by a SB during the months of (e) October to May, and (f) June to September. The synoptic flow directions were determined by examining mean sea level pressure maps and represent the following: 360° = N flow, 315° = NW, 270° = W, 225° = SW, 180° = S, 135° = SE, 90° = E, 45° = NE, and 0° = light and variable.

Under light and variable flow (0°), the distributions of onset times tend to lie between the earlier times of offshore flow and the later times of onshore flow. The onset times range from 2 to 9 hours after sunset during the MC months, and from 0 to 7 hours after sunset during the PC months (Figs. 5.3a-b). Most events under light and variable flow during the PC months followed a sea breeze and tended to have earlier onset times (Figs. 5.3d,f). Meanwhile, very little distinction was found between the SB and No SB onset times during the MC months (Figs. 5.3c,e).

The magnitude of the pressure gradient generally had little impact on the land-breeze onset time. There is some indication that stronger offshore flow led to earlier onset times and stronger onshore flow led to later onset times (not shown). However, the relationships are generally weak and not noteworthy.

Tables 5.1 and 5.2 provide a summary of the statistical distributions of land-breeze onset times based on a clustering of the MSLP flow regimes and sea-breeze occurrences for the MC and PC months. Table 5.1 shows the onset time results for land breezes during the MC months and Table 5.2 shows the onset time results for land breezes during the PC months. In addition, a visual supplement to Tables 5.1 and 5.2 is provided in Fig. 5.4, which contains box plots of the statistical distributions of land-breeze onset times for the MC (Fig. 5.4a) and PC months (Fig. 5.4b).

These tables and figure are designed to provide forecasters with a qualitative range of expected onset times based on the time of year, flow regime, and sea-breeze occurrence. Categories with small sample sizes should not be given much credence when estimating onset times. As a result, Fig. 5.4 does not include box plots of flow categories having sample sizes less than 10 events. Forecasters should also be aware of the large amount of variability in onset times under certain categories, particular for onshore and shore-parallel flow regimes during the MC months. Additional studies are required to obtain more precision in the land-breeze onset times.

Table 5.1. A summary of statistical properties of the land-breeze onset times (hours after sunset) under various surface flow regimes during the MC months of October to May. The onset times are categorized based on the sea-breeze (SB) occurrence or absence, and surface synoptic flow according to mean sea level pressure charts.

October to May: SB during preceding afternoon							
Surface Synoptic Flow	***Median Onset time***	***50% of events***	***80% of events***	***Min***	***Max***	***St. Dev.***	***Sample Size***
Offshore (NW/W/SW)	2.5	1.1 to 4.3	0.3 to 4.9	0.0	5.5	1.7	43
Onshore (NE/E/SE)	6.4	4.5 to 9.4	3.1 to 10.7	1.8	12.3	3.1	18
Shore-Parallel (S/N)	5.5	2.4 to 6.4	0.9 to 7.5	0.7	10.4	2.7	18
Light & Variable	4.8	3.8 to 6.1	3.3 to 7.5	1.9	8.0	1.8	18
October to May: No SB during preceding afternoon							
Surface Synoptic Flow	***Median Onset time***	***50% of events***	***80% of events***	***Min***	***Max***	***St. Dev.***	***Sample Size***
Offshore (NW/W/SW)	3.1	2.6 to 3.4	0.9 to 4.3	0.2	4.4	1.3	12
Onshore (NE/E/SE)	7.0	5.2 to 9.3	3.2 to 11.4	2.7	13.1	2.9	53
Shore-Parallel (S/N)	5.5	Sample size too small*	Sample size too small*	2.2	13.7	4.0*	7*
Light & Variable	6.4	3.4 to 7.5	2.7 to 8.7	2.5	9.2	2.5	11

*The percentile ranges were excluded for sample sizes less than 10. Use the standard deviation with caution for categories with such small sample sizes.

Table 5.2. A summary of statistical properties of the land-breeze onset times (hours after sunset) under various surface flow regimes during the PC months of June to September. The onset times are categorized based on the sea-breeze occurrence or absence, and the surface synoptic flow according to mean sea level pressure charts.

June to September: SB during preceding afternoon

Surface Synoptic Flow	*Median Onset time*	*50% of events*	*80% of events*	*Min*	*Max*	*St. Dev.*	*Sample Size*
Offshore (NW/W/SW)	1.6	0.2 to 3.3	-0.2 to 4.0	-0.3	5.5	1.7	39
Onshore (NE/E/SE)	6.5	5.5 to 7.9	4.8 to 9.2	4.0	10.0	1.7	24
Shore-Parallel (S/N)	4.0	Sample size too small*	Sample size too small*	1.5	5.6	1.6*	8*
Light & Variable	4.2	2.8 to 4.6	0.8 to 5.4	0.4	6.7	1.7	19

June to September: No SB during preceding afternoon

Surface Synoptic Flow	*Median Onset time*	*50% of events*	*80% of events*	*Min*	*Max*	*St. Dev.*	*Sample Size*
Offshore (NW/W/SW)	5.4	Sample size too small*	Sample size too small*	2.4	7.1	2.4*	3*
Onshore (NE/E/SE)	7.7	6.0 to 8.6	5.3 to 10.3	4.1	11.7	2.1	17
Shore-Parallel (S/N)	5.3	Sample size too small*	Sample size too small*	4.4	7.6	1.5*	4*
Light & Variable	4.7	Sample size too small*	Sample size too small*	3.1	6.9	1.4*	6*

*The percentile ranges were excluded for sample sizes less than 10. Use the standard deviation with caution for categories with such small sample sizes.

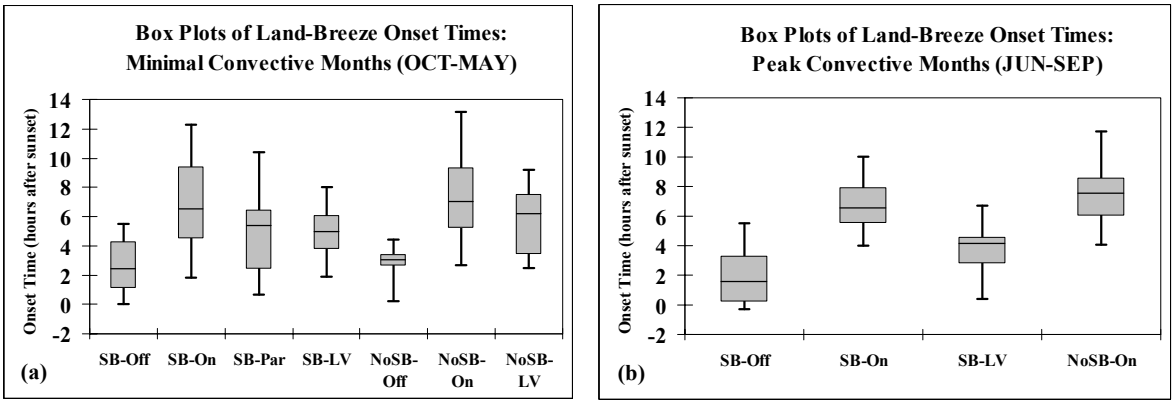

Figure 5.4. Box-plot distributions of the land-breeze onset times under various surface flow regimes during the (a) minimal convective months, and (b) peak convective months. The gray shading in each box plot indicates the onset times that occurred between the 1st and 3rd quartiles of the distribution, and the hatch marks at the top and bottom of each box plot indicate the maximum and minimum, respectively. Box plots are shown only for regimes that had a sample size of at least 10 occurrences according to the data provided in Tables 5.1 and 5.2. The flow regime notations are: SB occurrence with offshore synoptic flow (SB-Off), SB with onshore flow (SB-On), SB with shore-parallel flow (SB-Par), SB with light and variable flow (SB-LV), no SB with offshore flow (NoSB-Off), no SB with onshore flow (NoSB-On), and no SB with light and variable flow (NoSB-LV).

5.3 Land-Breeze Direction

The relationships between synoptic MSLP flow direction and the land-breeze direction are shown in Fig. 5.5 for the same categories as used in Fig. 5.3. By comparing Figs. 5.5a and b, it is evident that there were different distributions of favored land-breeze directions for the MC and PC months. During the MC months, the four favored relationships between the synoptic flow and the land-breeze direction were:

- NE or E MSLP flow yielding a NW land-breeze,
- SE MSLP flow yielding a SW land-breeze,
- SW MSLP flow yielding a SW land-breeze, and
- NW MSLP flow yielding a W land-breeze.

It is interesting to note that virtually no land breezes emanated from a NW direction when the synoptic flow was also from the NW. During the PC months of June to September, there were only two favored connections between the synoptic flow and land-breeze direction:

- SE MSLP flow yielding a W or SW land-breeze, and
- SW or W MSLP flow yielding a SW land-breeze.

Based on the frequency plots in Figs. 5.5a and b, there were other wind-shift combinations that occurred during the 7-year period of record; however, the most favorable scenarios are listed above, based on the distinct maxima in the plots.

By decomposing the frequency diagrams into events that did or did not have a sea breeze during the previous afternoon, one can see quite disparate distributions during the MC months (Figs. 5.5c and e). When a land breeze followed a sea breeze, the synoptic flow was primarily from the SW, and secondarily from the W or NW, whereas the land-breeze typically came from the SW or W (Fig. 5.5c). However, when a sea breeze did not precede the land breeze during the MC months, the synoptic flow was almost always from an onshore direction, with the favored regimes being SE flow with a SW land breeze, and NE to E flow with a NW land breeze (Fig. 5.5e). A secondary maximum occurred under NW flow leading to a W land breeze; however, for such a land-breeze front to occur, some onshore wind component must exist along the coast prior to the land-breeze frontal passage.

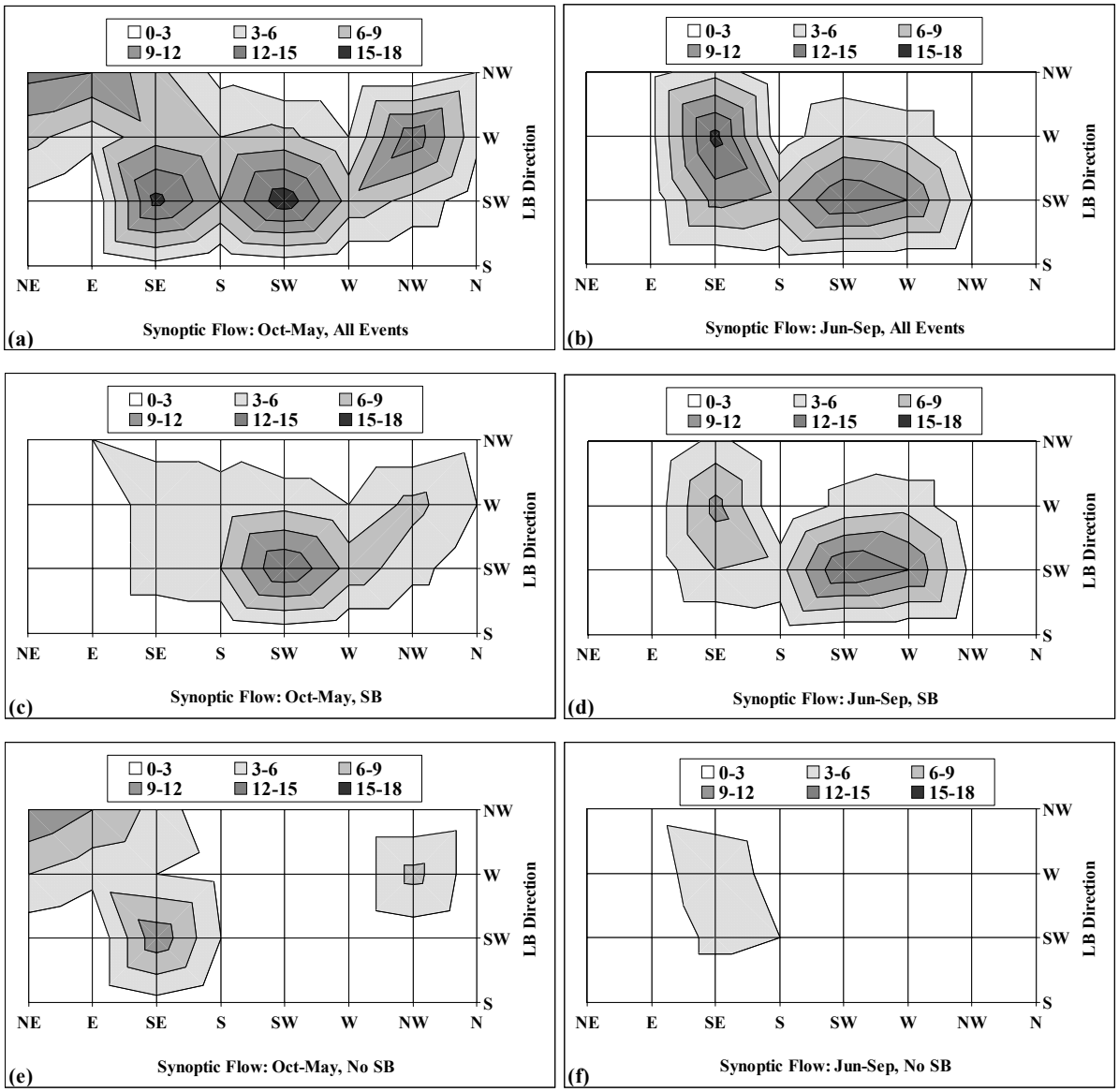

Figure 5.5. The frequency distributions of land-breeze directions from February 1995 to January 2002 as a function of the synoptic flow direction, based on a categorization of events into MC (October to May) versus PC months (June to September) and events with and without a preceding sea breeze (SB). All events are shown for the months of (a) October to May, and (b) June to September. Events preceded by a sea breeze are shown in (c) October to May, and (d) June to September. Events without a preceding sea breeze are shown in (e) October to May, and (f) June to September.

During the convective months, the two favored relationships between the synoptic and land-breeze directions were connected with those events preceded by a daytime sea breeze, particularly for the offshore synoptic directions (Figs. 5.5b and d). A very small secondary maximum of W and SW land breezes occurred under SE synoptic flow without a preceding sea breeze, but land-breeze events not preceded by a sea breeze during June to September were generally quite uncommon (Fig. 5.5f).

Finally, the light and variable synoptic flow (0° in Fig. 5.3) versus land-breeze direction are plotted in Fig. 5.6 for the MC months with and without a preceding sea breeze (MC, SB and MC, NoSB), and the PC months with and without a preceding sea breeze (PC, SB and PC, NoSB in Fig. 5.6). Under light and variable synoptic flow, the most favored land-breeze direction was W or SW during the MC months (October to May) and SW during the PC months (June to September). In addition, most land-breeze events under light and variable flow occurred with a preceding sea breeze, particularly during the PC months.

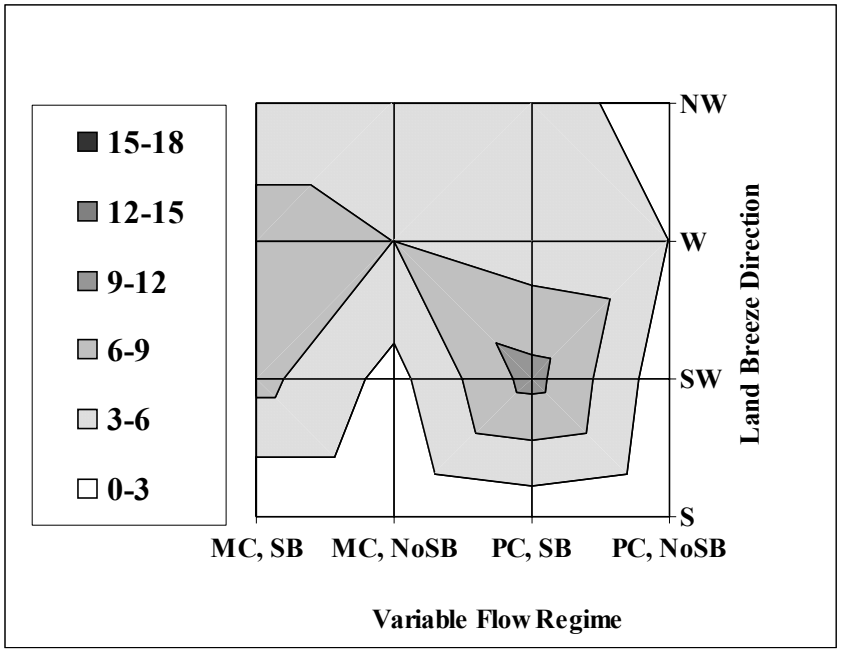

Figure 5.6. The frequency distribution of land-breeze directions from February 1995 to January 2002 for light and variable synoptic flow directions. The land breezes were grouped together for events that occurred during the MC months (October to May) preceded / not preceded by a sea breeze (MC, SB / MC, NoSB), and for events that occurred during the PC months (June to September) preceded / not preceded by a sea breeze (PC, SB / PC, NoSB).

6. Summary and Conclusions

This report presented the first multi-year, comprehensive observational study of land breezes over central Florida. Since very few observational studies have been conducted in the past to investigate land breezes in any location, this work represents a novel effort in defining the observational characteristics of land breezes, and their frequency of occurrence throughout the year.

6.1 Data Sources and Case Studies

This comprehensive analysis was enabled by the high-resolution observational tower network over KSC/CCAFS. Five-minute observations of winds, temperature, and moisture at several vertical levels allowed for continuous tracking of convergent boundaries along the leading edge of land breezes during the night. These tower data, along with available 915-MHz DRWP data, were presented for five sample events during the spring of 2000. The events discussed in Section 3 illustrated the varying conditions under which land breezes occurred and the different structural characteristics of the land breezes. The land breezes formed under a variety of surface temperatures, with and without a sea breeze during the preceding afternoon, and had widely varying depths and onset times.

6.2 Methodology for Developing Composite Climatology

To develop a multi-year, composite climatology of land breezes across KSC/CCAFS, the tower data at 54 ft were interpolated to a high-resolution analysis grid every 5 minutes so that an objective algorithm could be developed to track these boundaries in both space and time. This algorithm was designed to identify wind-shift lines from onshore to offshore wind directions, and ensure that these boundaries moved from west to east towards the Florida east coast. Several criteria were established prior to analyzing the wind fields for a land breeze:

- All nights with precipitation, excessive cloud ceiling observations, or large pressure changes at TTS were removed from consideration for a land-breeze event.
- Nights that had a pressure trough with an amplitude greater than 1 mb were removed from consideration.
- Nights with average wind speeds at 54 ft greater than ~ 7 kt were removed from consideration.

These criteria were established based on the subjective analysis of seven months of data from October 1999 to April 2000, and the initial development of the land-breeze identification algorithm on these months. The initial criteria were important to prevent the algorithm from falsely identifying frontal passages or outflow boundaries as land breezes. Once the algorithm was tuned to prevent most false identifications of land breezes, these criteria and the algorithm were applied to all days in the data set from 1 February 1995 to 31 January 2002.

All events identified by the algorithm were validated through visual inspection. In addition, the occurrence/absence of a sea breeze during the afternoon preceding each land breeze was determined. The events that impacted Tower 313 were also analyzed to examine the vertical depth and structure of the land breezes.

Composite climatologies were developed separately for the MC months (October to May) and the PC months (June to September). For each event identified by the algorithm, the 5-minute meteorological observations were archived for all tower locations that experienced the land-breeze passage for ± 60 minutes of the passage. A composite of the average meteorological conditions at ± 60 minutes of the passage time was then constructed for land breezes emanating from different directions.

6.3 Composite Seven-Year Climatology Results

During the 7-year period of record, there were 393 total land-breeze events identified and validated, 248 during the MC months of October to May, and 145 during the PC months of June to September. A summary of the characteristics of land breezes from the 7-year climatology are given below:

- Fog occurrence: Fog was much more common at TTS during land breeze nights compared to non-land breeze nights, valid for all months of the year.

- Monthly occurrence: Land breezes were most common during the mid-spring and mid-summer months (April, May, July, and August), and least common in December and January.
- Monthly onset times: The average onset times were earliest from May to July (~ 4 to 5 hours after sunset) and latest from October to January (~ 6.5 to 8 hours after sunset).
- Monthly land-breeze direction: Land breezes came from the W or SW most frequently from April to August, while land breezes from the NW were most prevalent during October and November. During the winter months, land breezes were equally likely from the SW, W, and NW.
- Monthly pre-land-breeze direction: S to SE winds were most prevalent before the land-breeze passage during February, and from April to September. Meanwhile, N to NE winds were most common prior to land breezes in October and November. The winter months saw fairly even distributions of pre-land-breeze wind directions, except for February.

There were 264 events seen in the Tower 313 data over Merritt Island, which was used to compare the behaviors of deep land breezes (depth > 492 ft) versus shallow land breezes (depth < 492 ft). Regardless of the time of year, it was found that land breezes with deep circulations had an onset time about 4 hours earlier than shallow circulations (average onset time of ~ 4.5 versus 8.5 hours after sunset). Over 80% of deep events had sea breezes the preceding afternoon, whereas less than 40% of shallow land breezes had sea breezes preceding them, suggesting that early, deep-circulation land breezes may be composed primarily of retreating sea breezes. The shallow land breezes were probably separate features not connected with the afternoon sea breeze and may have been driven by thermal contrasts between land and water or a nocturnal drainage flow. Deep land breezes typically came from the W or SW and often followed a sea breeze from the previous afternoon, whereas shallow land breezes came from all directions, but particularly favored the NW direction during the cooler months.

The composite changes in various meteorological quantities at ± 60 minutes of the land-breeze passages indicated that the land breeze was a density-current feature during the cooler months (October to May). The 54-ft composite temperatures saw a clear decrease with the passage of the land breeze. However, due to the light nature of winds during land-breeze nights, the 6-ft temperatures often increased with the passage of a land breeze due to the mechanical mixing of the stronger winds, which break the low-level inversion near the surface. As a result, the near-surface stability typically decreases with the passage of a land breeze, especially during the cooler months.

During June to September, only the NW land breeze showed signs that it was a density current, whereas all other land-breeze directions showed virtually no sign of cooling with the frontal passage. Since sea breezes were most common during the summer months, these results further suggest that the land breeze was typically a retreating sea breeze during these months. The combination of earlier onset times during the summer, a high frequency of sea-breeze occurrence, and lack of temperature decrease suggested that the retreating (eastward-moving) sea breeze was the most common type of land breeze during the summer, especially in July and August when land and sea breezes were most prevalent.

6.4 Summary of Forecast Tools

Finally, several tools were created to help forecasters predict the occurrence, onset time, and direction/movement of land breezes under different surface synoptic surface flows. A flowchart was developed to help forecasters determine the qualitative chances of a land-breeze occurrence on a particular night, given that a set of meteorological conditions are first satisfied. If a land breeze is possible, then forecasters can refer to the tables and charts developed for the onset times and direction/movement based on the surface synoptic flow characteristics, time of year, and sea-breeze occurrence during the day.

With additional resources, the climatological charts and tables provided in Section 5 could be transitioned into an automated tool. The tool could be built into the Meteorological Interactive Data Display System or installed onto a separate PC located in the Range Weather Operations of the 45 WS. The automated climatological-based tool could quickly provide forecasters with guidance for land-breeze occurrence, timing, and direction of movement all in a single concise package.

6.5 Suggested Future Work

Future efforts to improve the robustness of the forecast tools could involve a more rigorous climatology and/or the incorporation of the results of this study into a high-resolution dynamical numerical weather prediction (NWP) model. The most rigorous methodology for the climatology is to classify the synoptic flow and sea-breeze occurrence for every day of the 7-year data base when the wind speeds, pressure patterns, cloud cover, and lack of precipitation met the pre-defined criteria. The probability of a land-breeze event under various regimes during this 7-year period could be obtained directly by calculating the ratios of the number of land breezes to the total number of days under each regime. To construct these probabilities, the classification of the daily synoptic flow regime could be done objectively; however, the classification of the daily sea-breeze occurrence would require a manual examination of an extensive amount of data for seven years.

Through the use of a high-resolution NWP model, future efforts could also involve an examination of the dynamical balances involved with selected land-breeze events. By modeling specific scenarios, one could obtain a better understanding of the driving mechanisms behind the various types of land breezes discussed in this report. Also, experiments could be conducted that vary the land-sea temperature contrasts and flow regimes to measure the impact that each have on land-breeze development. Furthermore, one could examine the utility of a high-resolution NWP model in predicting the occurrence, timing, and movement of land breezes to determine any skill the model may have.

7. References

Arritt, R. W., 1993: Effects of the large-scale flow on characteristic features of the sea breeze. *J. Appl. Meteor.,* **32,** 116-125.

Atkins, N. T., and R. M. Wakimoto, 1997: Influence of the synoptic-scale flow on sea breezes observed during CaPE. *Mon. Wea. Rev.,* **125,** 2112-2130.

Atkins, N. T., R. M. Wakimoto, and T. M. Weckwerth, 1995: Observations of the sea-breeze front during CaPE. Part II: Dual-Doppler and aircraft analysis. *Mon. Wea. Rev.,* **123,** 944-969.

Atkinson, B. W., 1981: Sea/Land Breeze Circulation. *Mesoscale Atmospheric Circulations,* Academic Press, 125-214.

Barnes, S. L., 1964: A technique for maximizing details in numerical weather map analysis. *J. Appl. Meteor.*, **3**, 396-409.

Case, J. L., 2001: Final report on the evaluation of the Regional Atmospheric Modeling System in the Eastern Range Dispersion Assessment System. NASA Contractor Report CR-2001-210259, Kennedy Space Center, FL, 147 pp. [Available from ENSCO, Inc., 1980 N. Atlantic Ave., Suite 230, Cocoa Beach, FL 32931.]

Dekate, M. V., 1968: Climatological study of sea and land breezes over Bombay. *Indian J. Met. Geophys.,* **19,** 421-442.

Kalnay, E., and Coauthors, 1996: The NCEP/NCAR Reanalysis Project. *Bull. Amer. Meteor. Soc.,* **77,** 437-471.

Kingsmill, D. E., 1995: Convection initiation associated with a sea-breeze front, a gust front, and their collision. *Mon. Wea. Rev.,* **123,** 2913-2933.

Laird, N. F., D. A. R. Kristovich, R. M. Rauber, H. T. Ochs III, and L. J. Miller, 1995: The Cape Canaveral sea and river breezes: Kinematic structure and convective initiation. *Mon. Wea. Rev.,* **123,** 2942-2956.

Lambert, W. C. and G. E. Taylor, 1998: Data quality assessment methods for the Eastern Range 915-MHz wind profiler network. NASA Contractor Report CR-1998-207906, Kennedy Space Center, FL, 49 pp. [Available from ENSCO, Inc., 1980 N. Atlantic Ave., Suite 230, Cocoa Beach, FL 32931.]

Lambert, W. C., 2001: Statistical short-range forecast guidance for cloud ceilings over the Shuttle Landing Facility. NASA Contractor Report CR-2001-210264, Kennedy Space Center, FL, 45 pp. [Available from ENSCO, Inc., 1980 N. Atlantic Ave., Suite 230, Cocoa Beach, FL 32931.]

Lambert, W. C., 2002: Statistical short-range guidance for peak wind speed forecasts on Kennedy Space Center/Cape Canaveral Air Force Station: Phase I results. NASA Contractor Report CR-2002-, Kennedy Space Center, FL, 39 pp. [Available from ENSCO, Inc., 1980 N. Atlantic Ave., Suite 230, Cocoa Beach, FL 32931.]

Sen Gupta, P. K., and K. C. Chakravortty, 1947: Land breeze at Calcutta (Alipore). *Sci. Notes Met. Dept. India,* **9,** 73-80.

Simpson, J. E., 1996: Diurnal changes in sea-breeze direction. *J. Appl. Meteor.,* **35,** 1166-1169.

Stephan, K., C. M. Ewenz, and J. M. Hacker, 1999: Sea-breeze front variations in space and time. *Meteor. Atmos. Phys.,* **70,** 81-95.

Taylor, G. E., M. K. Atchison, and C. R. Parks, 1990: The Kennedy Space Center Atmospheric Boundary Layer Experiment. Report No. ARS-90-120, ENSCO, Inc., Melbourne, FL, 229 pp. [Available from ENSCO, Inc., 1980 N. Atlantic Ave., Suite 230, Cocoa Beach, FL 32931.]

Wakimoto, R. M., and N. T. Atkins, 1994: Observations of the sea-breeze front during CaPE. Part I: Single Doppler, satellite, and cloud photogrammetry analysis. *Mon. Wea. Rev.,* **122,** 1092-1114.

Wheeler, M. M., M. K. Atchison, R. Schumann, G. E. Taylor, J. D. Warburton, and A. Yersavich, 1993: Analysis of rapidly developing fog at the Kennedy Space Center preliminary report, 56 pp. [Available from ENSCO, Inc., 1980 N. Atlantic Ave., Suite 230, Cocoa Beach, FL 32931.]

Wilson, J. W., and D. L. Megenhardt, 1997: Thunderstorm initiation, organization, and lifetime associated with Florida boundary convergence lines. *Mon. Wea. Rev.,* **125,** 1507-1525.

Zhong, S., and E. S. Takle, 1992: An observational study of sea- and land-breeze circulation in an area of complex coastal heating. *J. Appl. Meteor.,* **31,** 1426-1438.

Zhong, S., and E. S. Takle, 1993: The effects of large-scale winds on the sea–land-breeze circulations in an area of complex coastal heating. *J. Appl. Meteor.,* **32,** 1181-1195.

List of Abbreviations and Acronyms

Term	Description
45 WS	45th Weather Squadron
AMU	Applied Meteorology Unit
CCAFS	Cape Canaveral Air Force Station
DRWP	Doppler Radar Wind Profiler
E	East
FAR	False Alarm Rate
KSC	Kennedy Space Center
MC	Minimal Convective
MCO	Orlando, FL 3-letter station identifier
MHz	Mega-Hertz
MLB	Melbourne, FL 3-letter station identifier
MSLP	Mean Sea Level Pressure
N	North
NCAR	National Center for Atmospheric Research
NCEP	National Centers for Environmental Prediction
NE	Northeast
No SB	No Sea Breeze
NW	Northwest
NWP	Numerical Weather Prediction
PC	Peak Convective
POD	Probability of Detection
QC	Quality Control
S	South
SB	Sea Breeze
SE	Southeast
SW	Southwest
TTS	Shuttle Landing Facility, FL 3-letter station identifier
UTC	Universal Time Coordinated
W	West

NOTICE

Mention of a copyrighted, trademarked or proprietary product, service, or document does not constitute endorsement thereof by the author, ENSCO, Inc., the AMU, the National Aeronautics and Space Administration, or the United States Government. Any such mention is solely for the purpose of fully informing the reader of the resources used to conduct the work reported herein.